A singular perturbation study of the Rolie-Poly model

Yuriko Renardy and Michael Renardy

Department of Mathematics, 460 McBryde Hall, 225 Stanger Street, Virginia Tech, Blacksburg, VA 24061-0123

Abstract

A singular perturbation analysis for the Rolie-Poly model is presented for the limit of large relaxation time. The model describes entangled linear polymer melts and time scales for a Rouse time and reptation time. First, the case of the Rouse time approaching zero, is named the nonstretching model, and the addition of a solvent model gives the small parameter to be the ratio of the retardation time to the slow reptation time. This analysis is instructive in formulating the perturbation analysis for the full Rolie-Poly model without the solvent, where the small parameter is the ratio of Rouse time to reptation time. The resulting formulae elucidate the characteristic features of thixotropic yield stress fluids, including yield stress hysteresis, delayed yielding and long term persistence of a decreased viscosity after cessation of flow. Two fundamental initial value problems are solved: startup of shear flow and cessation of shear flow. The scalings lead naturally to simplified dynamical systems that describe regimes of fast, slow and yielded dynamics, and show how the combination of these regimes can be used to describe the entire flow evolution.

Keywords: Rolie-Poly model, thixotropic yield stress fluid, singular perturbation
PACS: 83.60.La
2000 MSC: 76A10

1. Introduction

Thixotropic yield stress fluids display characteristics that cannot be explained by "simple" yield stress models like the Bingham or Herschel-Bulkley model, such as yield stress hysteresis, delayed yielding, and long term persistence of a decreased viscosity even after cessation of flow. In the literature,

this is often modeled by introducing a structure parameter, on which viscosity and yield stress depend, and which evolves on a slow time scale. On the other hand, some models of viscoelastic fluids display similar characteristics. These models do not, strictly speaking, have a yield stress, but they show a viscosity jump by several orders of magnitude at a critical shear stress; this is sometimes referred to as "apparent" yield stress behavior. The slow time scale is in this case given by a relaxation time which is long relative to other time scales.

It has been suggested [3] that the difference between "true" and "apparent" yield stress fluids is one of degree rather than principle. On the other hand, Larson [7] has recently tried to distinguish "ideal" thixotropic behavior from thixotropic features resulting from viscoelasticity. Regardless of such philosophical differences, we believe that viewing entangled polymers or wormlike micelles as perturbations of thixotropic yield stress fluids provides insights into their behavior and may suggest new approaches to both theoretical and experimental study. Asymptotic studies provide a more complete qualitative insight into the mechanisms underlying the dynamics of model fluids than can be obtained from purely numerical results, and they are particularly useful for problems involving highly disparate space and time scales which are hard to resolve numerically. For instance, studies of the PEC (partially extending strand convection) model of [6], combined with a Newtonian solvent, have led to analytical formulas for startup and cessation of homogeneous shear flows [11, 9].

The view of polymeric fluids as complex yield stress fluids also suggests new types of experiments. In this paper, an important focus of the analysis is the prediction of delayed yielding. In an experiment of constant imposed stress, the apparent yield stress decreases as the time of the experiment is increased. This is delayed yielding and is well documented for a suspension, i.e. ketchup [4]. We do not know of analogous experiments for polymers. Nevertheless, manifestations of delayed yielding are evident, for instance in stress overshoots. If shear rate rather than stress is imposed, then the stress required to achieve a given shear rate decreases with time, leading to an overshoot in the measured stress. Such overshoots are, for instance, shown in [8]. As we shall discuss in more detail below, transient shear banding is also a manifestation of delayed yielding. Other aspects which would be worthy of further experimental study include the evolution of apparent viscosity during relaxation to equilibrium after cessation of shear flow, and the detailed evolution of shear bands as time evolves. The insights gained from the

asymptotic studies provide specific guidance what to look for and what to expect. We note that there is considerable uncertainty in the literature about the magnitude of convective constraint release. As we shall see, thixotropic behavior is particularly sensitive to this effect.

In prior work [11], the limit of large relaxation time is studied for Larson's [6] Partially Extending Strand Convection (PEC) model, which was originally proposed as a model for entangled polymers, but has more recently been modified to describe wormlike micelles [13]. This multiple time scale asymptotic analysis succeeds in extracting useful predictions for yield stress hysteresis, delayed yielding, and thixotropy. The main impact of this work lies in the promotion of a method of analysis for transient evolution, rather than "validation" of a specific model. The PEC model is a prototype which is particularly simple to analyze, and the natural followup question is whether this approach can be utlized for more complicated models. On the one hand, for many thixotropic yield stress fluids such as pastes and suspensions, microstructural models which are simple enough to be amenable to much analysis seem hard to come by at this point in time. On the other hand, the theory of entangled polymers is better developed, and it is reasonable to attempt an analysis similar to [11]. The goal of this paper is such an analysis for the Rolie-Poly model. This model has recently gained popularity because it can predict transient shear banding, even in situations where the steady shear stress vs. shear rate behavior is monotone [1, 2]. We link this observation to delayed yielding below.

The Rolie-Poly model is first described in [8]. There are two relaxation times: the reptation time τ_d and the Rouse time τ_R. The stress tensor is given by $\mathbf{T} = G\mathbf{C}$, where $\mathbf{C}$ is a conformation tensor satisfying the constitutive equation

$$\dot{\mathbf{C}} - (\nabla \mathbf{v})\mathbf{C} - \mathbf{C}(\nabla \mathbf{v})^T = -\frac{1}{\tau_d}(\mathbf{C} - \mathbf{I}) - \frac{2(1 - \sqrt{3/\operatorname{tr}\mathbf{C}})}{\tau_R}(\mathbf{C} + \beta(\frac{\operatorname{tr}\mathbf{C}}{3})^\delta(\mathbf{C} - \mathbf{I})). \tag{1}$$

We focus on homogeneous flows; thus, the material time derivative of $\mathbf{C}$ reduces to the ordinary time derivative $\dot{\mathbf{C}}$. The convective constraint release (CCR) coefficient β and the exponent δ are dimensionless model parameters. The ratio $\epsilon = \tau_R/\tau_d$ is small, and this motivates our asymptotic analysis for small ϵ.

The dimensionless variables are obtained by scaling time with τ_R, and stress with G: $\mathbf{T}^* = \mathbf{T}/G$, $t^* = t/\tau_R$, $\nabla^* \mathbf{v}^* = \tau_R \nabla \mathbf{v}$. Hereafter, the asterisks

are dropped, to obtain:

$$\dot{\mathbf{C}} - (\nabla \mathbf{v})\mathbf{C} - \mathbf{C}(\nabla \mathbf{v})^T = -\epsilon(\mathbf{C} - \mathbf{I}) - 2(1 - \sqrt{3/\operatorname{tr}\mathbf{C}})(\mathbf{C} + \beta(\frac{\operatorname{tr}\mathbf{C}}{3})^\delta(\mathbf{C} - \mathbf{I})). \tag{2}$$

Our analysis below is based on asymptotics exploiting smallness of ϵ. A natural question is how small ϵ actually is for realistic fluids. For most of our numerical examples, we use $\epsilon = 0.001$, which was used in [1] on the basis of the width of the stress plateau in actual data. On the other hand, as pointed out by Wang [14] in a response to [1], "molecular" estimates for ϵ are larger by about one order of magnitude. This points to a discrepancy between the model and actual fluids which is yet to be resolved. Whatever more correct model eventually emerges will have to account for the smaller value of yielded to unyielded viscosity that is present in the actual data. On the other hand, if ϵ is indeed larger, then deviations between the asymptotic analysis and actual behavior become more significant. While the asymptotic results retain some qualitative relevance, the behavior of the full equations shows noticable deviations. We shall comment on some of these differences below.

A starting point for studying the full Rolie-Poly model is the simpler "nonstretching" version that is also introduced in [8], where a limit $\tau_R \to 0$ is taken in such a way that $\operatorname{tr}\mathbf{C} \to 3$ at the same rate at which $\tau_R \to 0$. Specifically, this model is obtained by taking the trace in (1):

$$\begin{aligned} \frac{d}{dt}(\operatorname{tr}\mathbf{C}) &= 2\operatorname{tr}((\nabla\mathbf{v})\mathbf{C}) - \frac{1}{\tau_d}(\operatorname{tr}\mathbf{C} - 3) \\ &\quad -\frac{2}{\tau_R}(1 - \sqrt{\frac{3}{\operatorname{tr}\mathbf{C}}})(\operatorname{tr}\mathbf{C} + \beta(\frac{\operatorname{tr}\mathbf{C}}{3})^\delta(\operatorname{tr}\mathbf{C} - 3)), \end{aligned}$$

setting $\operatorname{tr}\mathbf{C} = 3 + \tau_R\Delta$, and ignoring all terms of order τ_R. This yields

$$0 = 2\operatorname{tr}((\nabla\mathbf{v})\mathbf{C}) - \Delta, \tag{3}$$

and substitution in (1), neglecting terms which vanish as $\tau_R \to 0$, leads to the nonstretching Rolie-Poly model,

$$\dot{\mathbf{C}} - (\nabla\mathbf{v})\mathbf{C} - \mathbf{C}(\nabla\mathbf{v})^T = -\frac{2}{3}\operatorname{tr}((\nabla\mathbf{v})\mathbf{C})(\mathbf{C} + \beta(\mathbf{C} - \mathbf{I})) - \frac{1}{\tau_d}(\mathbf{C} - \mathbf{I}). \tag{4}$$

If the nonstretching model is taken as describing the complete stress tensor, it cannot account properly for the behavior at high shear rates; for this reason,

a Newtonian term is added to the constitutive equation, so that the extra stress tensor is

$$\mathbf{T} = G\mathbf{C} + \eta(\nabla\mathbf{v} + (\nabla\mathbf{v})^T). \tag{5}$$

The dimensionless equations are written in terms of a stress scaled with G, time scaled with the retardation time η/G, and the appropriate small parameter is $\epsilon = \eta/(G\tau_d)$. Thus, in dimensionless form, the extra stress tensor is $\mathbf{T} = \mathbf{C} + \nabla\mathbf{v} + (\nabla\mathbf{v})^T$. The constitutive equation is

$$\dot{\mathbf{C}} - (\nabla\mathbf{v})\mathbf{C} - \mathbf{C}(\nabla\mathbf{v})^T = -\frac{2}{3}\,\mathrm{tr}\,((\nabla\mathbf{v})\mathbf{C})(\mathbf{C} + \beta(\mathbf{C} - \mathbf{I})) - \epsilon(\mathbf{C} - \mathbf{I}). \tag{6}$$

Section 2 concerns the time-dependent behavior of the nonstretching model in the limit of small ϵ. The startup of shear flow under a prescribed shear stress is of fundamental importance; distinct regimes of fast, slow and yielded dynamics are found, as in the PEC model [11]. If the imposed shear stress is small enough, the initial fast dynamics transitions to slow dynamics and reaches an unyielded equilibrium. For large imposed stress, fast dynamics transitions to yielded dynamics, and a yielded equilibrium is reached. There is an intermediate range, however, where delayed yielding occurs because there is a transition from fast to slow dynamics, but no equilibrium is reached in slow dynamics. Instead, there is ultimately another transition to fast dynamics, followed by yielded dynamics. This delayed yielding occurs even if the constitutive curve for steady shear is monotone. The steady flow that is ultimately reached is yielded, but yielding occurs after a long time. If the shear stress is slightly inhomogeneous, as is inevitable in a real device, this inhomogeneity is magnified in the time needed to yield, and as a result, some layers yield later than others until the entire depth is fully yielded. This scenario manifests itself as transient shear bands [1, 2, 10]. We note that in prior literature, transient shear banding has sometimes been explained on the basis of a stability analysis, which is based on eigenvalues obtained after linearizing around a time dependent flow. However, this approach is open to question, since stability of time dependent flow can not generally be deduced from eigenvalues (see e.g. Example 3.3.7 in [5]). Just like our analysis here, a rigorous justification rests upon a separation of time scales, i.e. the growth of instabilities would have to be on a faster scale than the variation of the base flow. As an example of the connection between delayed yielding and transient shear banding, we cite the numerical computation of transient shear banding in Figure 1 of [10] . This figure is for the

nonstretching model with $\beta = 0.8$. According to our analysis below, delayed yielding occurs for imposed stresses between 0.6124 and 0.7319. The imposed stress value for Figure 1 is 0.7, which is near the upper end of our calculated window. Hence, delayed yielding is indeed expected from our analysis with a delay that is large relative to the retardation time but still small relative to the time τ_d. This is exactly in agreement. The formation of transient shear bands when the imposed stress or, as in [10], the initial condition, is slightly inhomogeneous, is the result of a corresponding variation in the delay time.

The cessation of shear flow is an important transient problem, where the initial state is an established steady shear flow, and the imposed shear stress is removed. In this case, we find, as in [11], that the motion comes to a stop quickly, but $\mathbf{C}$ relaxes back to its equilibrium value of $\mathbf{I}$ over a slow time scale. The result of this is thixotropic behavior. Compared to the PEC model, the Rolie-Poly model is much less thixotropic. This is a result of convective constraint release: For the PEC model, molecular orientation relaxes only on the slow reptation time scale. Convective constraint release allows partial relaxation of orientation on the fast time scale.

Section 3 provides a similar analysis for the stretching Rolie-Poly model. We first focus on the case $\delta = 0$, which is accessible to a fully analytical treatment. The results of the analysis show analogies to the nonstretching case. Section 4 discusses the case of nonzero δ. The results are very similar to $\delta = 0$, expect at high shear rates and shear stresses well above the yield threshold. The behavior is interpreted in terms of analysis.

2. The nonstretching Rolie-Poly model

The nonstretching Rolie-Poly model can be thought of as a twin to the PEC model studied in [11]. In the PEC model, we have $\beta = 0$, and instead there is a linear combination of $\mathbf{C}$ and $\mathbf{I}$ in the ϵ-term. The nonstretching Rolie-Poly with $\beta = 0$ is equivalent to the PEC model with (in the notation of [11]) $\alpha = 0$. In shear flow, we have

$$\mathbf{C} = \begin{pmatrix} C_{11} & C_{12} & 0 \\ C_{12} & C_{22} & 0 \\ 0 & 0 & C_{22} \end{pmatrix}, \tag{7}$$

and, with κ denoting the shear rate, we get

$$\dot{C}_{11} \;=\; 2\kappa C_{12} - \frac{2}{3}\kappa C_{12}((1+\beta)C_{11} - \beta) - \epsilon(C_{11} - 1),$$

$$
\begin{aligned}
\dot{C}_{12} &= \kappa C_{22} - \frac{2}{3}(1+\beta)\kappa C_{12}^2 - \epsilon C_{12}, \\
\dot{C}_{22} &= -\frac{2}{3}\kappa C_{12}((1+\beta)C_{22} - \beta) - \epsilon(C_{22} - 1).
\end{aligned}
$$

If the total shear stress τ is prescribed, then $\kappa = \tau - C_{12}$ (recall our nondimensionalization, which sets the Newtonian part of the viscosity equal to 1).

The equations combine to yield

$$
\frac{d}{dt}(C_{11} + 2C_{22} - 3) = -(\frac{2}{3}\kappa C_{12}(1+\beta) + \epsilon)(C_{11} + 2C_{22} - 3). \tag{8}
$$

Therefore $C_{11} + 2C_{22} = 3$ for all time if this is the case initially; this is why the model is called "nonstretching". Henceforth, we focus on the evolution of C_{12} and C_{22}.

2.1. Steady shear flow

For steady shear flow, we have

$$
\begin{aligned}
\kappa C_{22} - \frac{2}{3}(1+\beta)\kappa C_{12}^2 - \epsilon C_{12} &= 0, \\
-\frac{2}{3}\kappa C_{12}((1+\beta)C_{22} - \beta) - \epsilon(C_{22} - 1) &= 0.
\end{aligned}
$$

The first equation is solved for κ, which results in

$$
\kappa = \frac{3C_{12}\epsilon}{3C_{22} - 2(1+\beta)C_{12}^2}. \tag{9}
$$

This is used in the second equation, which is then solved for C_{12} to obtain

$$
C_{12} = \pm\sqrt{\frac{3}{2}}\sqrt{C_{22} - C_{22}^2}. \tag{10}
$$

The expression for κ now becomes

$$
\kappa = \pm\frac{\sqrt{\frac{3}{2}}\sqrt{C_{22}(1 - C_{22})}\epsilon}{C_{22}((1+\beta)C_{22} - \beta)}. \tag{11}
$$

There are three distinct features:

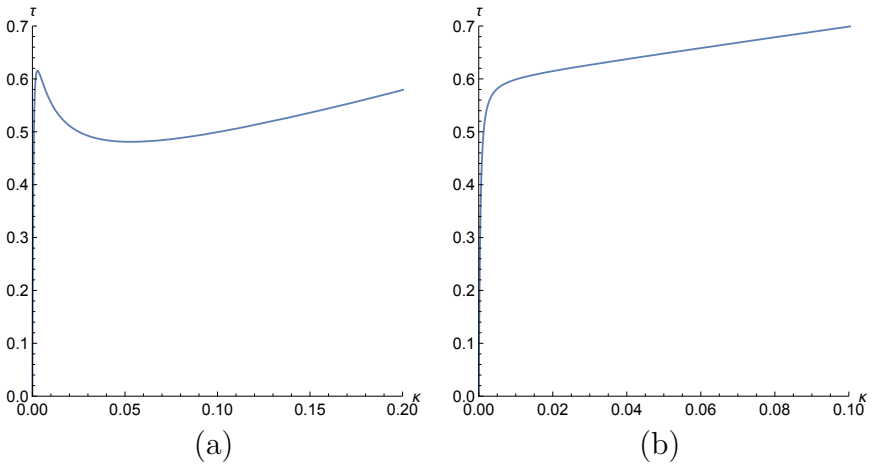

Figure 1: Steady flow curves for $\epsilon = 0.001$ and (a) $\beta = 0.1$, (b) $\beta = 1.5$.

1. Physically relevant steady flows exist for C_{22} in the range where the quantity under the square root and the denominator are both positive:

$$1 \geq C_{22} > \beta/(1+\beta).$$

   As C_{22} varies from 1 to $\beta/(1+\beta)$, κ varies from 0 to $\pm\infty$ and C_{12} varies from 0 to $\pm\sqrt{3\beta/2}/(1+\beta)$.
2. In the range $0 \leq C_{22} < \beta/(1+\beta)$, there exist solutions for which κ and C_{12} have opposite signs. These are an artifact of the model and will not be discussed further.
3. The elastic shear stress C_{12} goes through a maximum when $C_{22} = 1/2$, while the shear rate κ is a monotone function of C_{22}. Hence the model has a nonmonotone shear stress versus shear rate curve if $1/2$ is in the interval $(\beta/(1+\beta), 1)$, i.e. if $\beta < 1$; it is monotone for $\beta \geq 1$. For $\beta < 1$, and sufficiently small ϵ, the total shear stress $\tau = C_{12} + \kappa$ has a maximum at a shear rate of order ϵ and a minimum at a shear rate of order $\sqrt{\epsilon}$.

Figure 1 shows the steady flow curve for $\epsilon = 0.001$ and for (a) $\beta < 1$ at 0.1, and (b) $\beta > 1$, at 1.5. The non-monotone curve in (a) has two increasing branches where solutions may be observed, and the decreasing portion where solutions are unstable.

2.2. Fast dynamics in the nonstretching case

We begin by addressing the startup of shear flow from rest ($\mathbf{C} = \mathbf{I}$), under an imposed constant shear stress τ. The shear rate satisfies $\kappa = \tau - C_{12}$, and the initial condition is $C_{12} = 0$, $C_{22} = 1$. If ϵ is small, the initial transient is approximated by setting $\epsilon = 0$ in the governing equations. This regime is called fast dynamics. The strain γ is defined as the integral $\int_0^t \kappa(s)\, ds$. The equations for fast dynamics become

$$\begin{aligned} \frac{dC_{12}}{d\gamma} &= C_{22} - \frac{2}{3}(1+\beta)C_{12}^2, \\ \frac{dC_{22}}{d\gamma} &= -\frac{2}{3}C_{12}((1+\beta)C_{22} - \beta). \end{aligned} \tag{12}$$

Let $q = C_{12}/C_{22}$, so that the two equations of (12) are replaced by

$$\frac{dq}{d\gamma} = 1 - \frac{2}{3}\beta q^2. \tag{13}$$

Next, the initial condition is $q(0) = 0$; hence, the solution is

$$q(\gamma) = \sqrt{\frac{3}{2\beta}}\tanh(\sqrt{\frac{2\beta}{3}}\gamma). \tag{14}$$

Now, we can replace C_{12} by qC_{22} in the second equation of (12), and solve for C_{22}:

$$\begin{aligned} C_{22}(\gamma) &= \frac{\beta}{1+\beta - \operatorname{sech}(\sqrt{\frac{2\beta}{3}}\gamma)}, \\ C_{12}(\gamma) &= \frac{\sqrt{\frac{3\beta}{2}}\sinh(\sqrt{\frac{2\beta}{3}}\gamma)}{(1+\beta)\cosh(\sqrt{\frac{2\beta}{3}}\gamma) - 1}. \end{aligned}$$

Because of the imposed stress, the strain increases with time. There are two possible outcomes: Either the strain increases indefinitely or it stops increasing if the shear rate reaches zero. For $\gamma \to \infty$, $C_{22}(\gamma)$ approaches $\beta/(1+\beta)$. $C_{12}(\gamma)$ reaches a maximum value of $\sqrt{3/(2(2+\beta))}$ at

$$\gamma = \sqrt{\frac{3}{2\beta}}\ln(1+\beta - \sqrt{2\beta + \beta^2}), \tag{15}$$

and approaches $\sqrt{3\beta/2}/(1+\beta)$ from above. If, however, C_{12} reaches τ during this evolution, then the shear rate κ becomes zero, and, before this happens, κ becomes of order ϵ; the assumption of neglecting the order ϵ terms in the equations is no longer valid. This marks the end of fast dynamics with a transition to slow dynamics, to be described in the next section. Thus, there are two distinct scenarios:

1. If $\tau > \sqrt{3/(2(2+\beta))}$, then κ remains positive until $\gamma \to \infty$. The solution reaches yielded behavior where $C_{22} = \beta/(1+\beta)$ and $C_{12} = \sqrt{3\beta/2}/(1+\beta)$.
2. If $\tau < \sqrt{3/(2(2+\beta))}$, then C_{12} reaches τ, and a transition to slow dynamics occurs. The value of C_{22} at this point is

$$C_{22} = \frac{3(1+\beta) + \sqrt{3}\sqrt{3 - 2(2+\beta)\tau^2}}{3(2+\beta)}. \tag{16}$$

Thus far, the initial condition has been equilibrium. On the other hand, the analysis of thixotropy below requires the initial condition to be far from equilibrium. Specifically, we shall be interested in initial conditions $C_{12} = 0$, $C_{22} < 1$. These solutions are illustrated by the phase plane plots in the C_{12}-C_{22}-plane shown in Figure 2. We focus on the solution curves that start on the C_{22} axis between 0 and 1. In particular, the trajectories for the lower initial values of C_{22} achieve a smaller maximum value of C_{12}. Recall from the discussion above that this maximum value of C_{12} represents the threshold for immediate yielding. Indeed, we can show that if the initial condition for fast dynamics is the removal of applied stress $C_{12} = 0$, and $C_{22} = p$, then the maximum value of C_{12} is

$$\sqrt{\frac{3}{2(-\beta + 2(1+\beta)p)}}p. \tag{17}$$

For the thixotropy analysis below, we make use of the fact that this decreases with p in the interval $\beta/(1+\beta) < p < 1$.

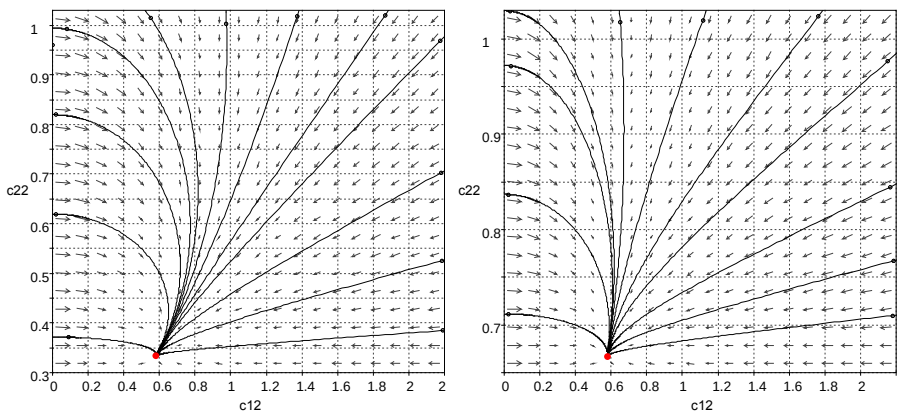

(a) (b)

Figure 2: Phase plane plot in the $C_{12} - C_{22}$ plane for the regime of fast dynamics defined by (12); (a) $\beta = 0.5$ and (b) $\beta = 2$. Vector arrows indicate direction of evolution toward the fixed points.

2.3. Slow dynamics for the nonstretching case

The slow dynamics regime is defined to be the evolution on the slow time scale, with shear rate κ of the same order as ϵ. Accordingly, $\kappa = \tilde{\kappa}\epsilon$, $C_{12} = \tau - \tilde{\kappa}\epsilon$, and $t = \tilde{t}/\epsilon$, where $\tilde{\kappa}$ and $\tilde{t}$ are simply rescaled variables. At the leading order,

$$\begin{aligned} 0 &= \tilde{\kappa} C_{22} - \frac{2}{3}(1+\beta)\tilde{\kappa}\tau^2 - \tau, \\ \frac{dC_{22}}{d\tilde{t}} &= -\frac{2}{3}\tilde{\kappa}\tau((1+\beta)C_{22} - \beta) - (C_{22} - 1). \end{aligned} \tag{18}$$

The first equation gives $\tilde{\kappa}$, which is substituted in the second equation to obtain a single equation,

$$\frac{dC_{22}}{d\tilde{t}} = \frac{3C_{22} - 3C_{22}^2 - 2\tau^2}{3C_{22} - 2(1+\beta)\tau^2}. \tag{19}$$

If $\tau^2 \leq 3/8$, there are two equilibrium points, representing unyielded states, given by the zeros of the numerator:

$$C_{22} = \frac{1}{2} \pm \frac{1}{2\sqrt{3}}\sqrt{3 - 8\tau^2}. \tag{20}$$

The denominator of (19) vanishes when

$$C_{22} = 2(1+\beta)\tau^2/3 =: C_{22}^s, \tag{21}$$

where the superscript denotes the singular value. Here, the slow curve (given by $C_{12} = \tau$) is tangent to a fast curve given by (12). In fact, with $C_{12} = \tau$, the right hand side of the first equation in (12) vanishes precisely at $C_{22} = 2(1+\beta)\tau^2/3$. The singular point also marks a change in the stability of the slow curve. If C_{22} decreases beyond the singular value C_{22}^s, fast curves move away from the slow curve rather than towards it, i.e. the slow curve is unstable.

The initial value upon entry to the slow curve is given by (16) and denoted C_{22}^i. The larger of the two equilibrium values given by (20) is denoted C_{22}^{eq}. Together with C_{22}^s, these values determine the subsequent evolution, and therefore it is important that the relative sizes be established. The advantage of this asymptotic analysis is clear at this stage, in extracting simplified formulas. Appendix A gives the calculation.

2.4. Startup of shear flow from rest for the nonstretching model

The results of the preceding sections and Appendix A yield the following behaviors in startup of shear flow from rest. Unyielded equilibrium is reached if the evolution on the slow manifold goes from C_{22}^i to C_{22}^{eq}, delayed yielding, with a delay time of order $1/\epsilon$, occurs if the evolution on the slow manifold goes from C_{22}^i to C_{22}^s, and immediate yielding occurs if slow dynamics is never reached.

2.4.1. Case $\beta < 1$

1. If $0 < \tau < \sqrt{3/8}$, the flow reaches unyielded equilbrium.
2. If $\sqrt{3/8} < \tau < \sqrt{3/(2(2+\beta))}$, delayed yielding occurs.
3. If $\tau > \sqrt{3/(2(2+\beta))}$, immediate yielding occurs.

2.4.2. Case $\beta > 1$

1. If $0 < \tau < \sqrt{3\beta/2}/(1+\beta)$, the flow reaches unyielded equilbrium.
2. If $\sqrt{3\beta/2}/(1+\beta) < \tau < \sqrt{3/(2(2+\beta))}$, delayed yielding occurs.
3. If $\tau > \sqrt{3/(2(2+\beta))}$, immediate yielding occurs.

These conditions for unyielded behavior, delayed yielding and immediate yielding in the (β, τ)-plane are shown in Figure 3.

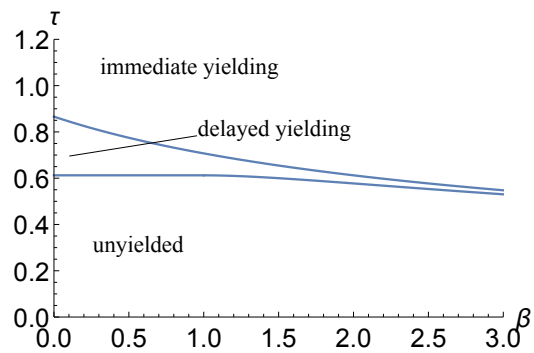

Figure 3: Regions of unyielded behavior, delayed yielding and immediate yielding in startup of shear flow for the nonstretching Rolie-Poly model.

2.5. Full numerical simulation for startup of shear flow for the nonstretching model

Figures 4 (a-d) show the time-dependent evolution of the shear rate for the CCR parameter $\beta = 0$ and increasing applied shear stress, from (a) $\tau = 0.6$ for unyielded flow, below the critical value of $\sqrt{3/8}$ (*cf.* Section 2.4.1). The shear rate for Figure 4 (a) settles to a value of approximately 0.001, which is comparable to $O(\epsilon)$ as predicted by the asymptotics, for $t > 10$. For $\sqrt{3/8} < \tau < \sqrt{3/4}$, Section 2.4.1 predicts delayed yielding, and this agrees with the simulations at $\tau = 0.7$ in Figure (b) and 0.8 in (c). Immediate yielding is predicted for $\tau > \sqrt{3/4}$, and this agrees with figure 4 (d) at $\tau = 0.9$. The time interval over which the shear rate is initially decreasing is, in fact, not of order $1/\epsilon$, but a much shorter interval, and thus this is not a delay. This plot is in the asymptotic regime; it remains the same at the smaller value of $\epsilon = 0.0001$.

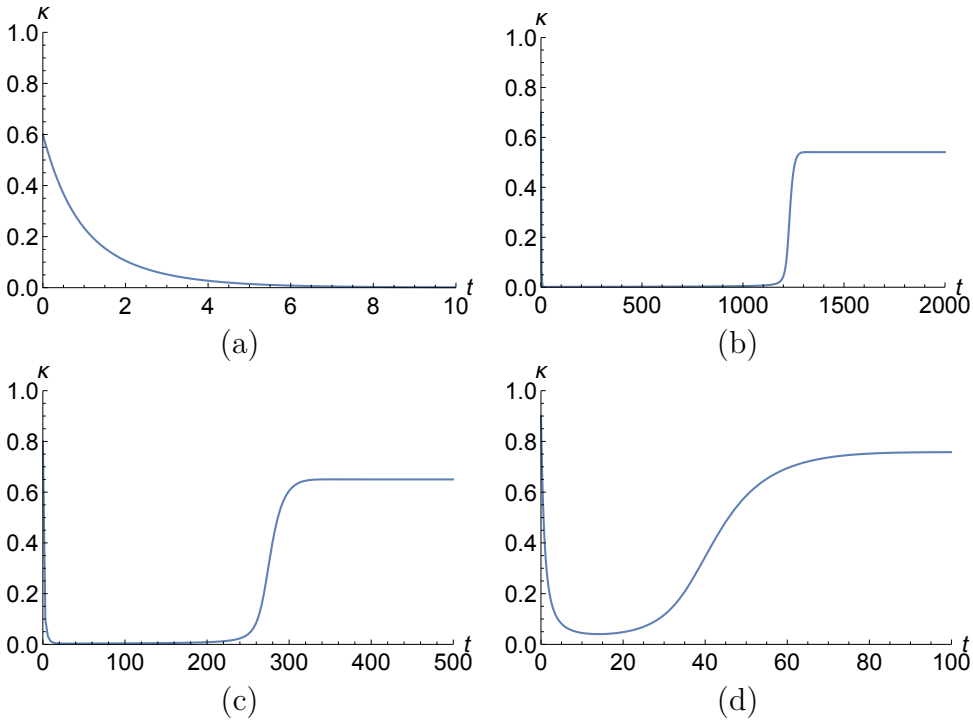

Figure 4: Evolution of shear rate for startup of shear flow for the nonstretching Rolie-Poly model, $\epsilon = 0.001$, $\beta = 0$. (a) $\tau = 0.6$, (b) $\tau = 0.7$, (c) $\tau = 0.8$, (d) $\tau = 0.9$.

For $\beta = 0.8$, the analysis of Section 2.4.1 predicts delayed yielding between $\tau = \sqrt{3/8} = 0.612$ and $\tau = 0.732$. This agrees well with the simulations at $\epsilon = 0.001$, which are not shown because they are similar in character to those shown in Figure 4.

Finally, the analysis of Section 2.4.2 for $\beta > 1$ is exemplified in the full numerical simulations of Figures 5 (a-d) at $\beta = 1.5$. Unyielded behavior is predicted for $\tau < 0.6$, and agrees with the simulation of Figure 5 (a) at $\tau = 0.59$, which settles to a shear rate of 0.007. Delayed yielding is predicted for $0.6 < \tau < 0.655$, and agrees with the plots (b) $\tau = 0.62$, and (c) 0.64. Immediate yielding is shown in (d) at $\tau = 0.67$. The critical stress values predicted by the analysis correspond well to the simulation results of Figure 5.

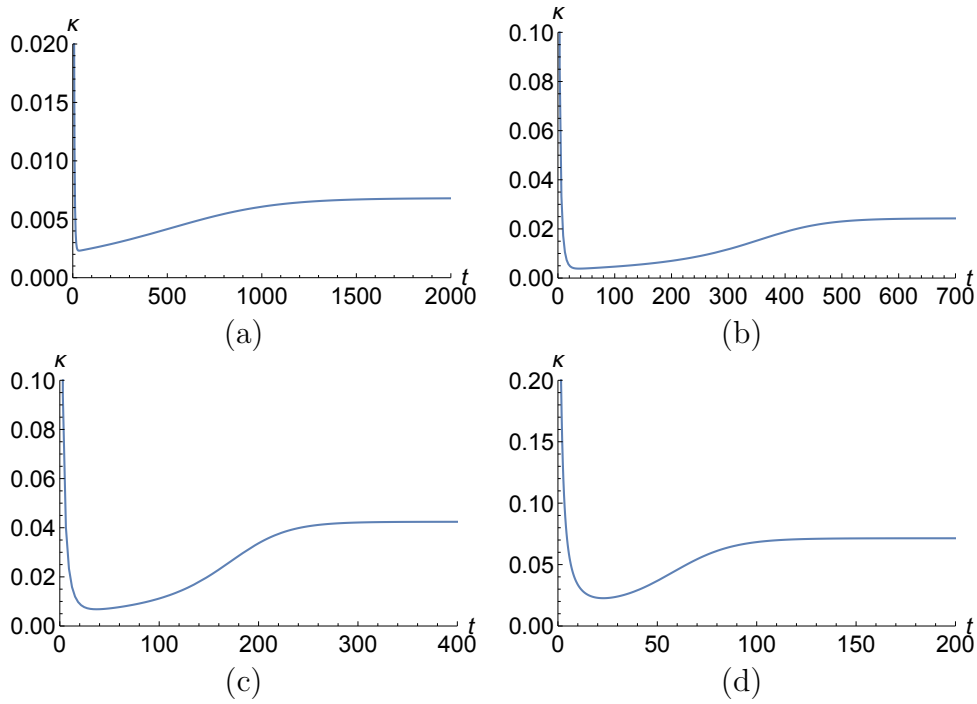

Figure 5: Evolution of shear rate for startup of shear flow for the nonstretching Rolie-Poly model, $\epsilon = 0.001$, $\beta = 1.5$. (a) $\tau = 0.59$, (b) $\tau = 0.62$, (c) $\tau = 0.64$, (d) $\tau = 0.67$.

2.6. Yielded dynamics and unyielding for the nonstretching moddel

The fast dynamics (12) has the fixed point $C_{22} = C_{22}^0 = \beta/(1+\beta)$, $C_{12} = C_{12}^0 = \sqrt{3\beta/2}/(1+\beta)$, which represents yielded steady flow. To predict details of the evolution after yielding, in particular the unyielding process when stress is reduced, a more detailed analysis of the vicinity of this fixed point is necessary. This is presented in Appendix B. The analysis shows the fixed point to be stable if $\tau > \sqrt{3\beta/2}(1+\beta)$.

If the initial condition is yielded flow, with a sudden ramping down of the applied stress, then Appendix B shows that the solution either settles to a new steady yielded flow corresponding to the new τ or leaves yielded dynamics via fast dynamics and subsequently enters slow dynamics to unyield over a time of order $1/\epsilon$.

2.7. Thixotropy

Let us consider in more detail the unyielding along the slow manifold. Specifically, we assume the applied stress has been reduced to zero. For

zero imposed stress, slow dynamics as given by (18) reduces to $\tilde{\kappa} = 0$ and $dC_{22}/d\tilde{t} = 1 - C_{22}$. That is, C_{22} is slowly increasing from $\beta/(1+\beta)$ to its equilibrium value of 1. Now at some point we reimpose a small stress τ. On the slow manifold, for small τ, we have approximately $\tilde{\kappa} = \tau/C_{22}$, i.e. $\kappa = \epsilon\tau/C_{22}$. This yields an apparent viscosity of $\tau/\kappa = C_{22}/\epsilon$. As C_{22} increases from $\beta/(1+\beta)$ back to 1, this apparent viscosity is slowly increasing. We note that the thixotropy is much less pronounced than it is for the PEC model; unless β is very small, the change in apparent viscosity during unyielding (from $\beta/((1+\beta)\epsilon)$ to $1/\epsilon$) is only by a factor of order 1 rather than several orders of magnitude as in [9].

If we reimpose a larger shear stress, the fluid might yield again. In the discussion of fast dynamics above, we saw that the threshold for immediate yielding depends on the initial value of C_{22}. The lower this initial value is, the smaller the stress required to induce immediate yielding. If immediate yielding does not occur and there is a transition to slow dynamics, the value of C_{22} at which this happens also decreases with decreasing initial value of C_{22}. That is, if delayed yielding occurs, the delay time will decrease as the initial value of C_{22} decreases.

During the unyielding process, the fluid therefore "effectively" has a viscosity and yield stress that increase gradually with aging.

3. The full Rolie-Poly model with $\delta = 0$

The full Rolie-Poly model (2) is too complicated to allow for analytically tractable solutions in general. However, the case $\delta = 0$ affords a simplification and is presented in this section. The nonstretching version of Section 2 is based on taking the limit $\tau_R \to 0$, leaving only τ_d as a timescale. This necessitated the introduction of a retardation time in order to create a second timescale. In contrast, the full Rolie-Poly model already has two timescales, with ratio $\epsilon = \tau_R/\tau_d$. A retardation term would create a third timescale and is not included to avoid masking the main effects of τ_R and τ_d. One consequence of not having a retardation term is the occurrence of step strains in the fast dynamics, which will be discussed below.

3.1. Steady shear flow asymptotics

The full steady shear flow equations at a prescribed shear stress $C_{12} = \tau$ are, from (2):

$$2\kappa C_{12} - \epsilon(C_{11} - 1) - 2(1 - \sqrt{3/(C_{11} + 2C_{22})})(C_{11} + \beta(C_{11} - 1)) = 0,$$

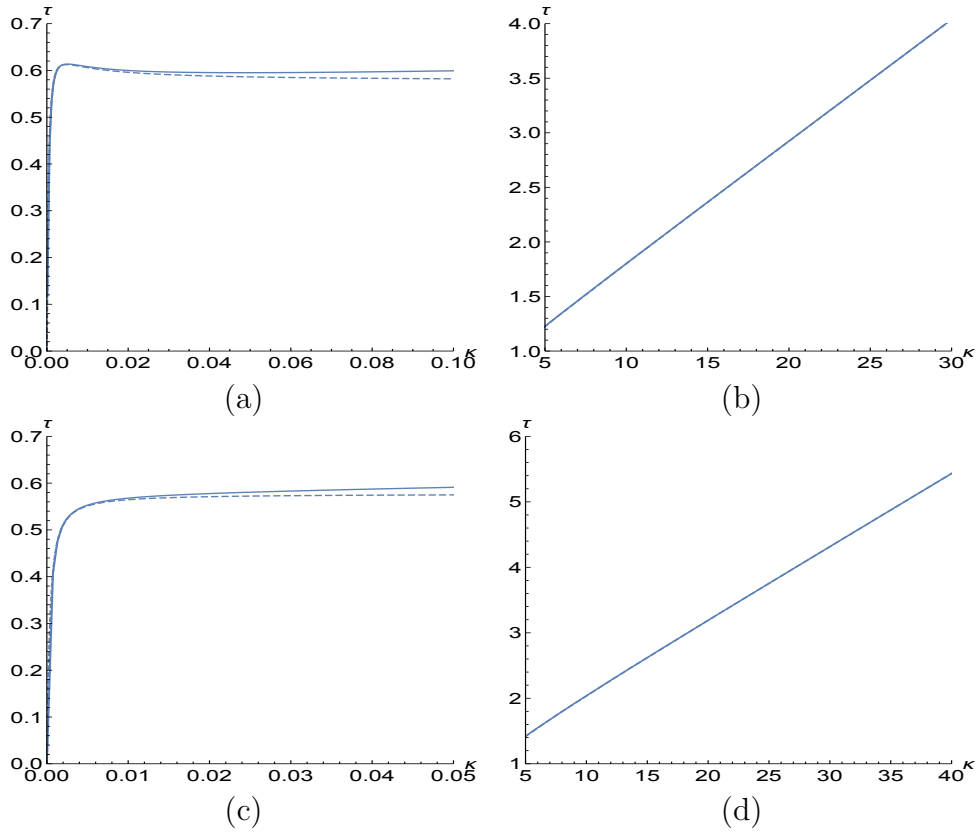

Figure 6: Steady flow curve for the full Rolie-Poly model, $\epsilon = 0.001$, $\delta = 0$. (a) $\beta = 0.5$, small shear rate, (b) large shear rate; (c) $\beta = 2$, small shear rate, (d) large shear rate. The dashed curves are from the asymptotic analysis for small ϵ.

$$\kappa C_{22} - \epsilon C_{12} - 2(1 - \sqrt{3/(C_{11} + 2C_{22})})(1 + \beta)C_{12} = 0,$$
$$-\epsilon(C_{22} - 1) - 2(1 - \sqrt{3/(C_{11} + 2C_{22})})(C_{22} + \beta(C_{22} - 1)) = 0. \quad (22)$$

The solid curves in Figure 6 show the exact steady flow curves for $\beta = 0.5$ and $\beta = 2$. The behavior of the steady flow curves in the limit of small ϵ is calculated next. There are two separate parts to the flow curve: an "unyielded" part where both the shear rate κ and $\operatorname{tr}\mathbf{C} - 3$ are of order ϵ, corresponding roughly to parts (a) and (c) of the figure, and a "yielded" part where C_{22} is close to $\beta/(1 + \beta)$, corresponding roughly to parts (b) and (d) of the figure.

Consider the unyielded part, where both the shear rate κ and the molecular stretch $\operatorname{tr}\mathbf{C} - 3$ are of order ϵ. We therefore set $C_{11} = 3 - 2C_{22} + \epsilon d$,

$\kappa = \epsilon\tilde{\kappa}$, where d and $\tilde{\kappa}$ are scaled correction terms to be evaluated. The equations are truncated at order ϵ. This essentially retrieves the nonstretching formula (10) in Section 2. On the physically relevant branch, the shear rate increases from zero to infinity as C_{22} decreases from 1 to $\beta/(1+\beta)$. The shear stress goes through a maximum when $C_{22} = 1/2$, if β is less than 1. For $\beta > 1$, the shear stress is monotone. The limiting value at $C_{22} = \beta/(1+\beta)$ is $C_{12} = \sqrt{3\beta/2}/(1+\beta)$. As C_{22} approaches $\beta/(1+\beta)$, $\tilde{\kappa}$ tends to infinity, and the assumption that the shear rate is of order ϵ is no longer valid.

For C_{22} close to $\beta/(1+\beta)$, a different analysis is required. This is the yielded part of the steady flow curve . The last equation of (22) is utilized with $C_{22} = \beta/(1+\beta) + d$, where d is a correction term to be evaluated; $\operatorname{tr}\mathbf{C}$ is obtained, namely,

$$\operatorname{tr}\mathbf{C} = \frac{12(1+\beta)^4 d^2}{(2d(1+\beta)^2 - \epsilon + (1+\beta)d\epsilon)^2}. \tag{23}$$

This is substituted into the second equation of (22) to find:

$$\kappa = \frac{C_{12}\epsilon}{d(\beta + d + \beta d)}. \tag{24}$$

These expressions for κ and $\operatorname{tr}\mathbf{C}$ are inserted into the first equation in (22). For small ϵ and d, the leading order balance becomes

$$2C_{12}^2(1+\beta)^2(-2(1+\beta)^2 d+\epsilon)^2 - 3\beta(4(1+\beta)^4 d^2 + 4\beta(1+\beta)^2\epsilon d - \beta\epsilon^2) = 0. \tag{25}$$

Two conclusions are immediately evident:

1. A solution exists for $d > \epsilon/(2(1+\beta)^2)$. As d tends to $\epsilon/(2(1+\beta)^2)$, C_{12} approaches infinity. Moreover, we see from (24) that the viscosity C_{12}/κ approaches the limit $\beta/(2(1+\beta)^2)$. In the opposite limit, as d/ϵ approaches infinity, C_{12} approaches $\sqrt{3\beta/2}/(1+\beta)$.
2. A more careful analysis, which will be omitted here, shows that for $\beta < 1$, C_{12} assumes a minimum when d is of order $\sqrt{\epsilon}$, and d^2 is approximately $\epsilon\beta/((1-\beta)(1+\beta)^2)$.

The dashed curves in Figure 6 represent the asymptotic analysis above. The agreement with the exact results (solid curve) is evident; in the large shear rate regime, both curves coincide. Thus, the essential features are captured by the asymptotics.

3.2. Fast dynamics for startup

Consider the startup of shear flow. The shear stress C_{12} jumps from 0 to τ. That is, C_{12} is a Heaviside function, and $\dot{C}_{12}$ is a delta function. The jump in stress induces a jump in strain, i.e. the shear rate κ also becomes a delta function. The initial evolution is described by $\epsilon = 0$ in the full equation (2):

$$\begin{aligned}\dot{C}_{11} &= 2\kappa C_{12} - 2(1-\sqrt{3/\operatorname{tr}\mathbf{C}})(C_{11}+\beta(C_{11}-1)),\\ \dot{C}_{12} &= \kappa C_{22} - 2(1-\sqrt{3/\operatorname{tr}\mathbf{C}})(1+\beta)C_{12},\\ \dot{C}_{22} &= -2(1-\sqrt{3/\operatorname{tr}\mathbf{C}})(C_{22}+\beta(C_{22}-1)).\end{aligned} \tag{26}$$

We deduce from (26) that there is no jump in C_{22}. Moreover, the second equation gives κ, and the first equation leads to

$$\dot{C}_{11} = \frac{2C_{12}\dot{C}_{12}}{C_{22}} + ... = \frac{1}{C_{22}}\frac{d}{dt}(C_{12}^2) + ..., \tag{27}$$

where the dots indicate terms that do not include a delta function. By integrating this, we conclude that the jump in C_{11} is $1/C_{22}$ times the jump in C_{12}^2. If the motion starts from rest with a step increase of the shear stress to τ, then the initial condition is $C_{11} = 1+\tau^2$, $C_{12} = \tau$, and $C_{22} = 1$.

From this initial condition, there is continuous evolution with a fixed $C_{12} = \tau$. It follows that

$$\kappa = 2(1-\sqrt{3/\operatorname{tr}\mathbf{C}})(1+\beta)\tau/C_{22}. \tag{28}$$

We use this in the first equation of (26). Moreover, we introduce a new time variable u by setting $du/dt = 1-\sqrt{3/\operatorname{tr}\mathbf{C}}$. With

$$s = \operatorname{tr}\mathbf{C},$$

the equations transform to

$$\begin{aligned}\frac{dC_{22}}{du} &= -2(C_{22}+\beta(C_{22}-1)),\\ \frac{ds}{du} &= \frac{4}{C_{22}}(1+\beta)\tau^2 + 2(3\beta-(1+\beta)s).\end{aligned} \tag{29}$$

The first equation gives

$$C_{22} = \frac{\beta}{1+\beta} + c_1 e^{-2(1+\beta)u}, \tag{30}$$

and the initial condition $C_{22} = 1$ yields $c_1 = 1/(1+\beta)$. This is substituted in the second equation. With the initial condition $s = 3 + \tau^2$, we find

$$\begin{aligned} s = \frac{3\beta}{1+\beta} + \frac{2\tau^2(1+\beta)}{\beta} + \frac{3}{1+\beta} e^{-2(1+\beta)u} - \frac{\tau^2(2+\beta)}{\beta} e^{-2(1+\beta)u} \\ + \frac{2\tau^2(1+\beta)}{\beta^2} e^{-2(1+\beta)u} (\ln(1+\beta) - \ln(1+\beta e^{2(1+\beta)u}). \end{aligned} \tag{31}$$

Thus, only two possibilities arise:

1. s reaches the value 3 at a finite value of u. In that case, $\operatorname{tr}\mathbf{C} - 3$ and κ become zero at this point. We have a transition to slow dynamics, discussed in the next subsection.
2. If s does not reach the value 3, we have $C_{22} \to \beta/(1+\beta)$ and $s \to 3\beta/(1+\beta) + 2\tau^2(1+\beta)/\beta$ for $u \to \infty$. At this point, we have a transition to yielded dynamics.

The subsequent motion hinges on whether s as given by (31) does or does not reach the value 3 at a finite positive value of u. Unfortunately, it is difficult to determine this from (31) directly, and we pursue a different approach. We note that $s(0) > 3$. If the limit of s for $u \to \infty$ is less than 3, then s must definitely cross 3. This is the case if

$$\tau^2 < \frac{3\beta}{2(1+\beta)^2}. \tag{32}$$

If τ^2 is bigger than this value, then both $s(0)$ and $s(\infty)$ are bigger than 3. The only way in which s can reach 3 is if it goes through a minimum, and the value of the minimum is less than or equal to 3. We now look for the limiting case when the value of the minimum is exactly 3. If $s = 3$ and $ds/du = 0$, then we conclude from the second equation of (29) that

$$C_{22} = \frac{2}{3}(1+\beta)\tau^2. \tag{33}$$

We can now determine tha value of u for which this is the case and use it in the expression for s. The result is a quite lengthy expression depending on β

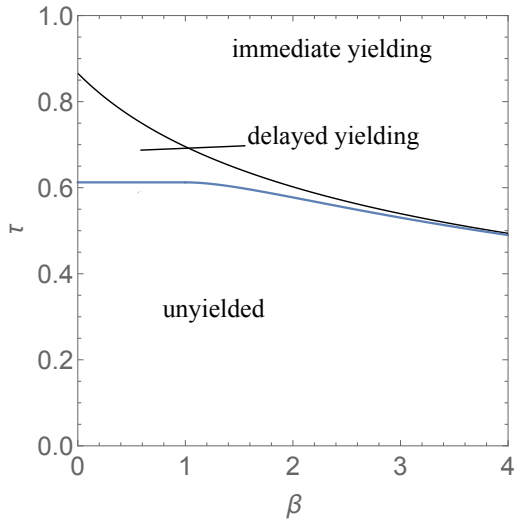

Figure 7: Regions of unyielded behavior, delayed yielding and immediate yielding for the full Rolie-Poly model, $\delta = 0$.

and τ, which we do not reproduce. Instead we show a contour plot showing the line where that expression is equal to 3.

The upper curve in Figure 7 is the line in the (β, τ) plane where the solution given by (31) reaches a minimum of 3; that is, below the curve s reaches 3, above it does not. The next section shows that the curve marks the boundary between immediate and delayed yielding. The lower curve in the plot is the boundary between delayed yielding and unyielded behavior. As shown next, with details given in Appendix C, this is the same as for the nonstretching Rolie-Poly model.

3.3. Slow dynamics

Unlike the nonstretching case, there is no tractable formula for C_{22}^i, which is the value of C_{22} where fast dynamics transitions to slow dynamics in the startup of shear flow. However, the essential qualitative features are obtained in the analysis presented in Appendix C. In summary, analogous results to the nonstretching case in Section 2.3 are obtained for the startup of steady shear flows:

1. If either $\beta < 1$ and $\tau < \sqrt{3/8}$ or $\beta \geq 1$ and $\tau < \sqrt{3\beta/2}/(1+\beta)$, slow dynamics leads to an unyielded equilibrium.

2. If $\beta < 1$, $\tau > \sqrt{3/8}$ or $\beta \geq 1$, $\tau > \sqrt{3\beta/2}/(1+\beta)$, but τ is still less than the value given by the upper curve in Figure 7, delayed yielding occurs.
3. If τ is larger than the value given by the upper curve in Figure 7, immediate yielding occurs.

3.4. Yielded dynamics

Yielded dynamics is examined by addressing the case when C_{22} is close to $\beta/(1+\beta)$. The details are given in Appendix D. If $\tau^2 > 3\beta/(2(1+\beta)^2)$, yielded dynamics settles to the steady shear flow. If $\tau^2 < 3\beta/(2(1+\beta)^2)$, then yielded dynamics at the steady shear flow is unstable, followed by a transition to unyielding. If a flow starts from a yielded steady shear flow at an imposed shear stress τ and then it is lowered to a new value τ, then the flow will remain yielded if $\tau^2 > 3\beta/(2(1+\beta)^2)$, but it will unyield and transition to slow dynamics if τ^2 is less than this value.

3.5. Thixotropy

Thixotropic behavior occurs in the same manner as the nonstretching model of Section 2. Suppose we start from a yielded shear flow and then reduce τ to zero. On the slow manifold, s is close to 3, κ is zero, but C_{22} grows from $\beta/(1+\beta)$ back to 1 only slowly, on a timescale of $1/\epsilon$. If we now reimpose a shear stress, then the initial jump of s will be equal to τ^2/C_{22}, which is larger than it would be if we started from equilibrium. Also, the shear rate is given by

$$\kappa = \frac{2(1-\sqrt{3/s})(1+\beta)+\epsilon}{C_{22}}\tau, \tag{34}$$

so the apparent viscosity τ/κ decreases with increasing s and decreasing C_{22}. On the slow manifold, according to (60), the apparent viscosity is

$$\frac{3C_{22} - 2(1+\beta)\tau^2}{3\epsilon}. \tag{35}$$

3.6. The case $\beta = 0$

So far, we have always assumed that $\beta > 0$. We conclude this section with a discussion of the special case $\beta = 0$. The nonstretching case, with the added Newtonian term, is equivalent to the PEC model discussed in [11]; we

note that the tensor denoted by $\mathbf{C}$ there is not the same as in this paper: our $\mathbf{C}$ would correspond to $\mathbf{C}/s$ in the notation of [11]. We now give a discussion of the stretching case.

The difference to the case of nonzero β is that the value of C_{22} in the yielded regime becomes of order ϵ. To focus on this regime, we investigate what happens when ϵ and C_{22} are small, and $s-3$ is not of order ϵ, but larger. For steady flow, we obtain the following simplified set of equations:

$$\begin{aligned} 2\kappa C_{12} - 2(1-\sqrt{\frac{3}{s}})s &= 0, \\ \kappa C_{22} - 2(1-\sqrt{\frac{3}{s}})C_{12} &= 0, \\ \epsilon - 2(1-\sqrt{\frac{3}{s}})C_{22} &= 0. \end{aligned}$$

We can solve for C_{12}, C_{22} and κ in terms of s. The result is

$$\begin{aligned} C_{22} &= \frac{\epsilon}{2(1-\sqrt{3/s})}, \\ C_{12}^2 &= \frac{\epsilon s}{4(1-\sqrt{3/s})}, \\ \kappa &= \frac{4C_{12}(1-\sqrt{3/s})^2}{\epsilon}. \end{aligned}$$

Thus the limiting viscosity at high shear rate ($s \to \infty$) is $\epsilon/4$. A minimum of shear stress is reached when $s = 27/4$; the corresponding shear rate and shear stress are $\kappa = \sqrt{1/\epsilon}$ and $C_{12} = \frac{9}{4}\sqrt{\epsilon}$.

To study yielded dynamics with an imposed shear stress τ of order 1, we set $s = \tilde{s}/\epsilon$, $C_{22} = c_{22}\epsilon$, and $\kappa = \tilde{\kappa}/\epsilon$. At leading order, we find the equations

$$\begin{aligned} \dot{\tilde{s}} &= 2\tilde{\kappa}\tau - 2\tilde{s}, \\ \dot{c}_{22} &= 1 - 2c_{22}, \\ \kappa c_{22} &= 2\tau. \end{aligned} \tag{36}$$

These equations have a stable fixed point at $c_{22} = 1/2$, $\tilde{s} = 2\tau^2$. Unyielding will not occur unless the shear stress is lowered to zero (more precisely, to $O(\sqrt{\epsilon})$).

Now we consider what happens during unyielding. We note that C_{22} obeys the equation

$$\dot{C}_{22} = \epsilon(1 - C_{22}) - 2(1 - \sqrt{\frac{3}{s}})C_{22}. \tag{37}$$

If we start with an initial value of order ϵ, then C_{22} will not grow beyond order ϵ until $s - 3$ becomes small, i.e. slow dynamics has been reached. During the slow phase of unyielding, C_{22} therefore grows from order ϵ back to its equilibrium value of 1, i.e. it changes by a factor of $1/\epsilon$ rather than a factor of order 1 as it did for nonzero β. Hence the model with $\beta = 0$ is much more thixotropic than the model with nonzero β.

4. The case of nonzero δ

In the previous section, we have focussed on $\delta = 0$, because it the most tractable case mathematically. On the other hand, Likhtman and Graham [8] advocate the choice $\delta = -0.5$ on the basis of a fit to a more elaborate molecular theory. In this section, we shall consider the case of nonzero δ. A nonzero value of δ is most important when $\operatorname{tr}\mathbf{C}/3$ is large, i.e. in the regime of high shear stress and shear rate. This will be evident in the analysis of steady shear flow below. On the other hand, as long as $\operatorname{tr}\mathbf{C}$ is not too much above 3, the effect of changing δ is relatively minor, as will be shown by the partial analysis as well as the numerical results below. Thus the dynamics of yielding and unyielding is only minimally affected by the choce of δ.

4.1. Steady shear flow

The steady shear flow equations are

$$\begin{aligned} -\epsilon(C_{22} - 1) - 2(1 - \sqrt{s/3})(C_{22} + \beta(\frac{s}{3})^{\delta}(C_{22} - 1)) &= 0, \\ \kappa C_{22} - \epsilon C_{12} - 2(1 - \sqrt{s/3})(1 + \beta(\frac{s}{3})^{\delta})C_{12} &= 0, \\ 2\kappa C_{12} - \epsilon(s - 3) - 2(1 - \sqrt{s/3})(s + \beta(\frac{s}{3})^{\delta}(s - 3)) &= 0. \end{aligned} \tag{38}$$

The first equation is solved for C_{22}:

$$C_{22} = \frac{\epsilon + 2\beta(s/3)^{\delta}(1 - \sqrt{3/s})}{\epsilon + 2(1 - \sqrt{3/s})(1 + \beta(s/3)^{\delta})}. \tag{39}$$

The second equation of (38) is solved for C_{12} and used in the third equation to obtain κ. This yields both C_{12} and κ as functions of s. Important qualitative aspects are pointed out next without reproducing the lengthy and complicated formulas. Close to equilibrium, s is close to 3, and $(s/3)^\delta$ is approximately 1. The slow dynamics of the previous section is therefore independent of δ. At the other extreme, large deformation means $s/3$ is large. If δ is positive, we obtain $C_{22} \sim 1$ in this limit, and the remaining equations simplify to

$$\kappa \sim 2\beta(\frac{s}{3})^\delta C_{12}, \quad 2\kappa C_{12} \sim 2\beta s(\frac{s}{3})^\delta.$$

This leads to

$$C_{12} \sim \sqrt{\frac{s}{2}}, \quad \kappa \sim \frac{\sqrt{2}\beta}{3^\delta} s^{1/2+\delta}.$$

Hence C_{12} is proportional to $\kappa^{1/(1+2\delta)}$, i.e. we have shear thinning behavior.

For $\delta = 0$, we noted in the previous section that the viscosity approaches the constant value $\beta/(2(1+\beta)^2)$ at large shear rates.

If δ is negative, then (39) leads to different behaviors depending on whether $(s/3)^\delta$ is large or small relative to ϵ. If s is large, but still small relative to $\epsilon^{1/\delta}$, then

$$C_{22} \sim \beta(s/3)^\delta. \tag{40}$$

We then find

$$\kappa\beta(s/3)^\delta \sim 2C_{12}, \quad 2\kappa C_{12} \sim 2s.$$

The result is a shear thinning behavior where κ is proportional to $s^{(1-\delta)/2}$, and C_{12} is proportional to $s^{(1+\delta)/2}$. On the other hand, if s is large relative to $\epsilon^{1/\delta}$, then C_{22} is close to $\epsilon/2$. The leading order balance in the remaining equations then becomes

$$\frac{\epsilon}{2}\kappa \sim 2C_{12}, \qquad 2\kappa C_{12} \sim 2s.$$

That is, the viscosity is constant, equal to $\epsilon/4$.

For the numerical simulations, we compare the values $\delta = -0.5$, $\delta = 0$ and $\delta = 0.5$. We focus on two values of β, one of which is chosen less than 1 and the other greater than 1; specifically we choose $\beta = 0.5$ and $\beta = 2$. Throughout, we set $\epsilon = 0.001$; this value was also chosen in [1] on the basis

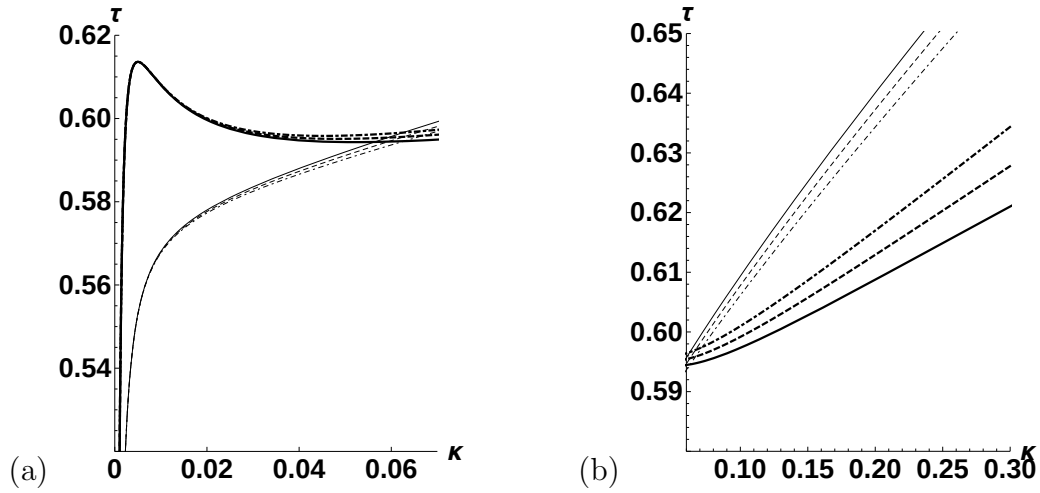

Figure 8: Steady flow curves for small shear rate and nonzero δ. $\delta = -0.5$, $\beta = 0.5$ (-) and 2.0 (—); $\delta = 0$, $\beta = 0.5$ (- - -) and 2.0 (- - -); $\delta = 0.5$, $\beta = 0.5$ (- · -) and 2.0 (- · -). (a) shear rate close to 0, (b) continuation up to shear rate 0.3.

of a fit to experimental data for polybutadiene reported in [12]. Figure 8 shows the behavior at low shear rates; (a) is on a scale close to zero shear rate and (b) is for slightly larger shear rate up to 0.3. As expected, there is little dependence on δ. For $\beta = 0.5$, the flow curve is nonmonotone, for $\beta = 2$ it is monotone, as predicted by the analysis in the preceding section.

For the behavior at large shear rate, we present $\beta = 0.5$; the case $\beta = 2$ is similar. Figure 9 shows results for $\delta = 0$, 0.5 and -0.5. For $\delta = 0$, (a) displays linear behavior (constant viscosity), while for $\delta = 0.5$ shear thinning is evident as predicted. For the negative exponent $\delta = -0.5$, Figure 9 (c-d) displays shear thinning over a wide range, but eventually the slope becomes constant in accordance with the foregoing analysis.

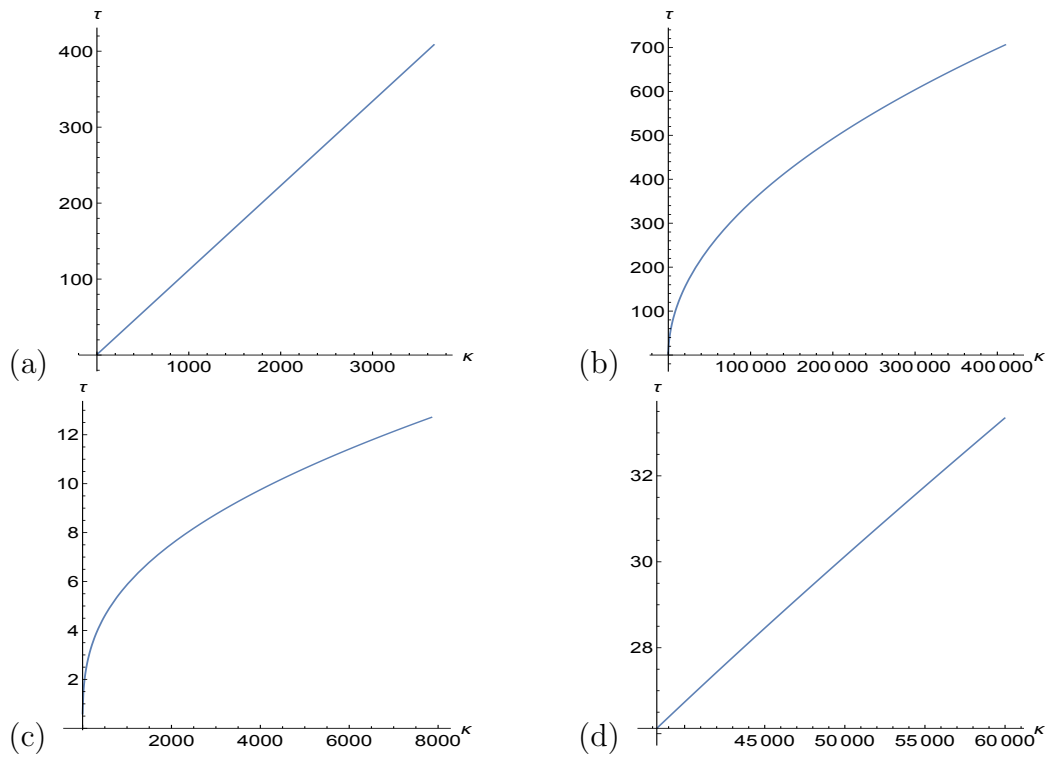

Figure 9: Steady flow curves for large shear rate, $\beta = 0.5$. (a) $\delta = 0$, the viscosity is constant. (b) $\delta = 0.5$, the fluid is shear thinning. (c) $\delta = -0.5$. The fluid is shear thinning over a wide range, but (d) eventually the viscosity becomes constant.

4.2. Analysis for nonzero δ

Since slow dynamics occurs when $\operatorname{tr}\mathbf{C}$ is approximately 3, it is not affected by the choice of δ. The equations of slow dynamics discussed in the previous section therefore remain the same, regardless of δ. We shall therefore focus on fast dynamics, obtained by setting $\epsilon = 0$ in the governing equations. The resulting equations are

$$\begin{aligned}
\frac{dC_{22}}{dt} &= -2(1-\sqrt{s/3})(C_{22}+\beta(\frac{s}{3})^{\delta}(C_{22}-1)),\\
0 &= \kappa C_{22} - 2(1-\sqrt{s/3})(1+\beta(\frac{s}{3})^{\delta})\tau,\\
\frac{ds}{dt} &= 2\kappa\tau - 2(1-\sqrt{s/3})(s+\beta(\frac{s}{3})^{\delta}(s-3)).
\end{aligned} \tag{41}$$

Getting a closed form solution of these equations is unlikely to be feasible. We can, however, discuss a number of qualitative results, which will be similar to those obtained for $\delta = 0$ above.

First, we discuss stationary solutions and their stability. Clearly, $s = 3$, $\kappa = 0$ is a stationary solution, corresponding to the limit of slow dynamics. Eliminating κ from the equations above, we find

$$\frac{ds}{dt} = 2(1 - \sqrt{s/3})(2\frac{\tau^2}{C_{22}}(1 + \beta(\frac{s}{3})^\delta) - (s + \beta(\frac{s}{3})^\delta(s - 3))). \tag{42}$$

We conclude that slow dynamics is attractive if $C_{22} > 2\tau^2(1+\beta)/3$, and loses its stability if $C_{22} < 2\tau^2/(1 + \beta)$. Not surprisingly, this is identical to the results for $\delta = 0$. We now look for other stationary points. From the first equation of (41), we find

$$C_{22} = \frac{\beta(s/3)^\delta}{\beta(s/3)^\delta + 1}. \tag{43}$$

By using this, and eliminating κ as before, we find the following condition for a stationary point

$$2\tau^2(1 + \beta(s/3)^\delta)^2 = \beta(s/3)^\delta(s - 3\beta(s/3)^\delta + \beta s(s/3)^\delta). \tag{44}$$

Solutions for $s < 3$ are unphysical, leading to opposite signs of τ and κ. For $s > 3$, the right hand side of the last equation is positive, and we find a unique value of τ^2 for any given s. As before, we shall refer to this stationary point as the yielded fixed point. On the basis of the analysis above, we expect the yielded fixed point to be stable for $s > 3$, and we shall show that this is indeed the case.

To simplify the algebra, we use a rescaled time variable defined by $d\tilde{t}/dt = 2(1 - \sqrt{s/3})$; for $s > 3$ this does not change the stability. In the rescaled time variable, we have the system

$$\begin{aligned} \frac{dC_{22}}{d\tilde{t}} &= -(C_{22} + \beta(s/3)^\delta(C_{22} - 1)), \\ \frac{ds}{d\tilde{t}} &= 2\frac{\tau^2}{C_{22}}(1 + \beta(s/3)^\delta) - (s + \beta(s/3)^\delta(s - 3)). \end{aligned} \tag{45}$$

The Jacobian matrix of this system is given by

$$\begin{pmatrix} a & b \\ c & d \end{pmatrix}, \tag{46}$$

where

$$
\begin{aligned}
a &= -1-\beta(s/3)^{\delta}, \\
b &= \beta(1-C_{22})(s/3)^{\delta}s^{-1}, \\
c &= -2(\tau/C_{22})^2(1+\beta(s/3)^{\delta}), \\
d &= -1-\beta\delta(s/3)^{\delta}(s-3)/s-\beta(s/3)^{\delta}+2\beta\delta\tau^2(s/3)^{\delta}/(C_{22}s). \qquad (47)
\end{aligned}
$$

For the yielded fixed point, we use the expressions for C_{22} and τ^2 as given by (43) and (44), and obtain

$$
\begin{aligned}
a+d &= -\frac{2s-3\beta\delta(s/3)^{\delta}+4\beta s(s/3)^{\delta}+2\beta^2 s(s/3)^{2\delta}}{s(1+\beta(s/3)^{\delta})}, \\
ad-bc &= 1+\delta-6\beta\delta s^{-1}(s/3)^{\delta}+2\beta(s/3)^{\delta}+\beta\delta(s/3)^{\delta}+\beta^2(s/3)^{2\delta} \qquad (48)
\end{aligned}
$$

It is easy to see that, as long as $s>3$, and δ is within the range $[-1,1]$, $a+d$ is negative, and $ad-bc$ is positive. This shows stability of the yielded fixed point.

In startup of shear flow, we can expect ultimate yielding if the imposed shear stress is larger than the maximum in the steady flow curve. As above for $\delta=0$, we can expect regimes of immediate and delayed yielding. It does not seem feasible to obtain an analytic expression for the boundary between these regimes. On the other hand, if τ is below the threshold for immediate yielding, $\operatorname{tr}\mathbf{C}/3$ will not become very large, and we can expect the effect of δ to be minor. Our numerical results below confirm this expectation.

In the limit $s=3$, (43) and (44) lead to

$$
C_{22}=\frac{\beta}{1+\beta}, \quad \tau^2=\frac{3\beta}{2(1+\beta)^2}, \qquad (49)
$$

identical to the result for $\delta=0$. We can expect unyielding if τ drops below this value. Let us now consider the situation where we start from an established yielded steady flow and there lower the imposed stress τ below this threshold. The dynamics will initially follow the fast dynamics until $s=3$ is reached and there is a transition to slow dynamics. As above, thixotropic behavior depends on the value of C_{22} that is reached when this transition to slow dynamics occurs. In the case $\delta=0$, the value of $C_{22}=\beta/(1+\beta)$ remained invariant under the fast dynamics, regardless of the evolution of s. This is no longer the case for nonzero δ. We can conclude from the first

equation of (41) that dC_{22}/dt always has a sign opposite to $C_{22} - c(s)$, where

$$c(s) = \frac{\beta(s/3)^\delta}{\beta(s/3)^\delta + 1}. \tag{50}$$

Initially, s is some value greater than 3, and $C_{22} = c(s)$. Since $C_{22}(0) = c(s(0))$ and dC_{22}/dt has a sign opposite to $C_{22} - c(s(t))$, it is easy to conclude that, and any time t, $C_{22}(t)$ must lie inside the closed interval formed by the values $\{c(s(t')), 0 \leq t' \leq t\}$. In particular, this precludes C_{22} from reaching its equilibrium value of 1. If the evolution of s is monotone, which is guaranteed at least for $\tau = 0$, then C_{22} will always be between its initial value and $c(3) = \beta/(1+\beta)$.

4.3. Full numerical simulation of startup of shear flow

Startup of shear flow is fundamental to initial value problems. The fluid is initially at rest, and for $t \geq 0$ a shear stress τ is imposed. Figure 10 (i) shows the evolution of the shear rate κ for $\epsilon = 0.001$, $\beta = 0.5$, $\delta = -0.5$, and τ in the range $0.6 \leq \tau < 1$. The value 0.6 is less than $\sqrt{3/8}$ (the value of the steady shear stress maximum), and the flow settles to an unyielded steady state. As τ is increased, delayed yielding occurs. The delay shortens with increasing τ, and eventually yielding becomes immediate. When compared with Figure 10 (ii) for $\delta = 0.5$, the effect of changing δ does not change the essential qualitative features.

Figure 11 shows the evolution for $\epsilon = 0.001$, $\beta = 2$, for (i) $\delta = -0.5$ and (ii) 0.5. Here, the maximum value of τ for unyielded steady flow is $\sqrt{3}/3 = 0.577$. Again we find delayed yielding in a window above this value. Comparison with the evolution in Figure 10 indicates that the change in β from 0.5 to 2 has more noticeable effect on the evolution scenario while the change in δ has a minor effect.

The numerical simulations presented so far utilize $\epsilon = 0.001$ because it is consistent with experimental data in [1] and the asymptotic analysis for small ϵ predicts the essential features of the solution. On the other hand, molecular theory links ϵ to the estimated number of entanglements per chain and suggest a larger value of ϵ for typical polymers, perhaps on the order of 0.01 [14]. The asymptotic theory becomes less applicable as ϵ is increased, for instance, the demarcation between monotone and nonmonotone behavior in steady flow shifts from $\beta = 1$ to smaller values of β, see e.g. [2]. However, at least qualitatively, some of the features apparent in the asymptotic analysis

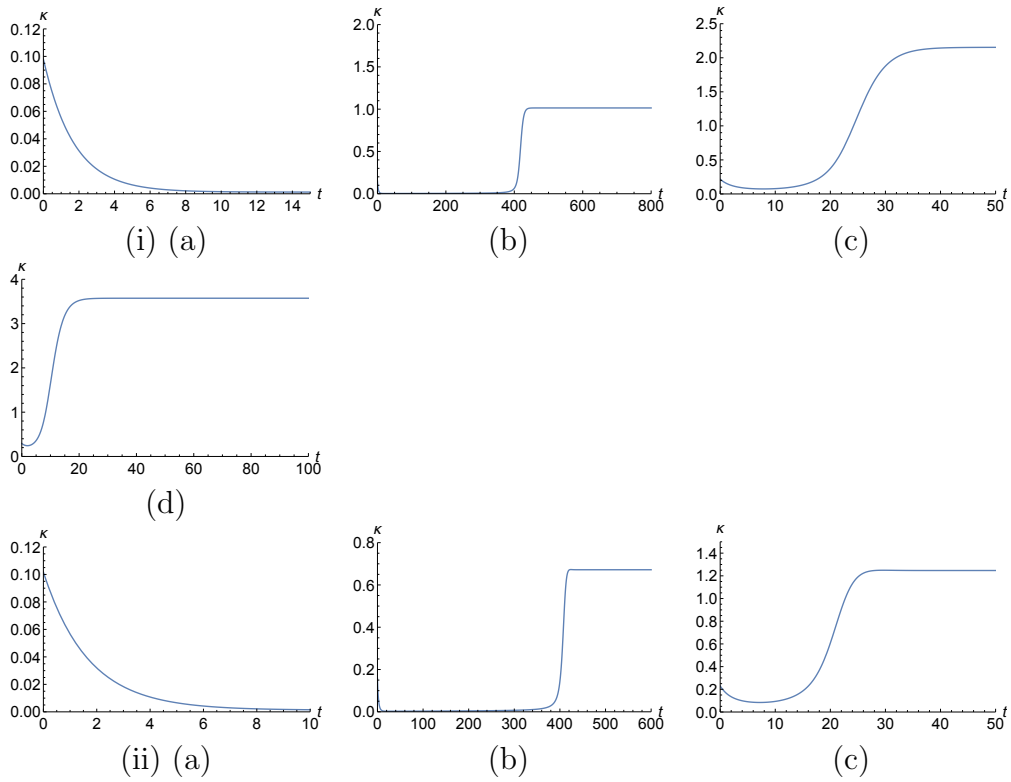

Figure 10: Evolution of shear rate for startup of shear flow, $\beta = 0.5$, $\epsilon = 0.001$, (i) $\delta = -0.5$: (a) $\tau = 0.6$, (b) $\tau = 0.7$, (c) $\tau = 0.8$, (d) $\tau = 0.9$. (ii) $\delta = 0.5$: (a) $\tau = 0.6$, (b) $\tau = 0.7$, (c) $\tau = 0.8$.

survive. Figure 12 shows delayed yielding for $\epsilon = 0.01$; the other parameters are the same as in Figure 10 (i).

4.4. Unyielding and thixotropy

We show one instance of unyielding from an established steady flow. For the parameters, we choose $\beta = 0.5$, $\delta = -0.5$ and $\epsilon = 0.001$. We start with steady flow at $\tau = 1$, corresponding to $s = 9.87979$ in the parameter representation discussed at the beginning of Section 4.1. We then instantaneously reduce the imposed shear stress to zero. The initial conditions after the instantaneous step strain are $C_{11} = 4.83155$ and $C_{22} = 0.21669$. Figure 13 shows the time evolution of $s = C_{11} + 2C_{22}$ and C_{22}. As expected from the analysis above for $\delta = 0$ (see Section 3.5), s relaxes quickly to 3, while C_{22} reaches its equilibrium value of 1 only on a timescale of order $1/\epsilon$.

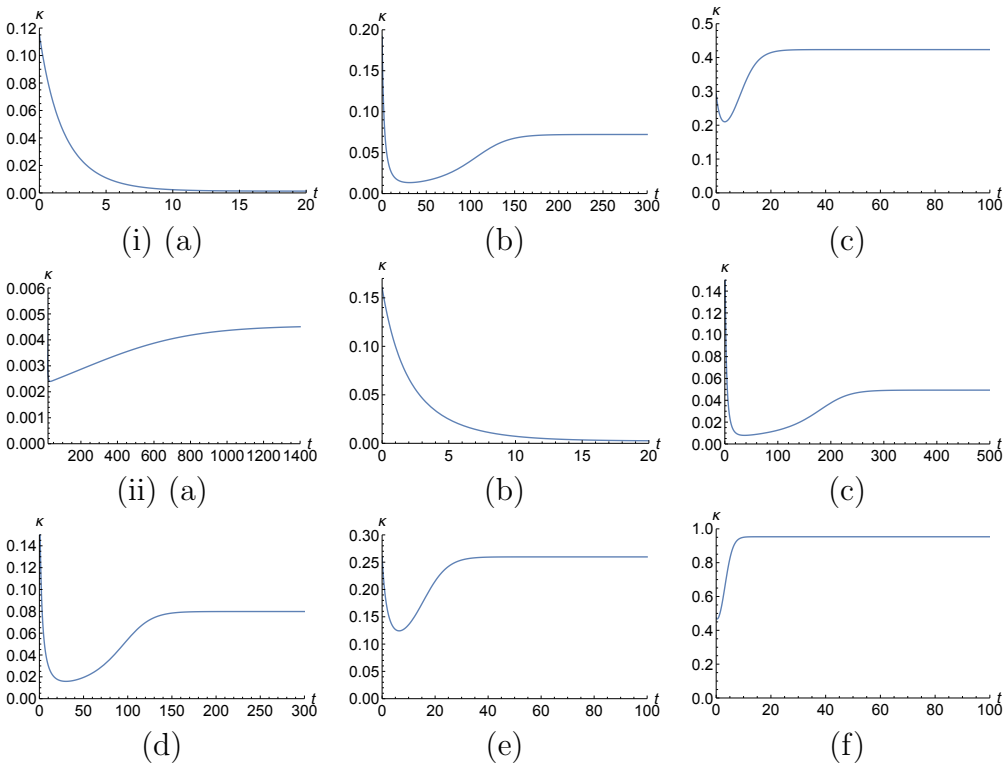

Figure 11: Evolution of shear rate for startup of shear flow, $\beta = 2$, $\epsilon = 0.001$, (i) $\delta = -0.5$: (a) $\tau = 0.5$, (b) $\tau = 0.6$,(c) $\tau = 0.7$. (ii) $\delta = 0.5$: (a) $\tau = 0.55$, and short time magnification in (b), (c) $\tau = 0.59$, (d) $\tau = 0.6$, (e) $\tau = 0.65$, (f) $\tau = 0.8$.

Conclusions

Startup of shear flow under an imposed shear stress and cessation of flow are of fundamental importance to understanding transient evolution of entangled polymeric melts. The mathematical modeling in the presence of two disparate time scales such as the Rouse time and reptation time can lead to behavior that is characteristic of thixotropic fluids. The framework for the mathematical analysis presented in this paper is successful in extracting simplified expressions for variables such as the evolution of the components of stress in limiting cases. The method is based on singular perturbation theory with multiple time scales. We have given a full asymptotic analysis of startup and cessation of homogeneous shear flow for the nonstretching Rolie-Poly model and for the full Rolie-Poly model when the exponent δ is zero. Partial analysis and numerical results for nonzero δ show similar dynamics.

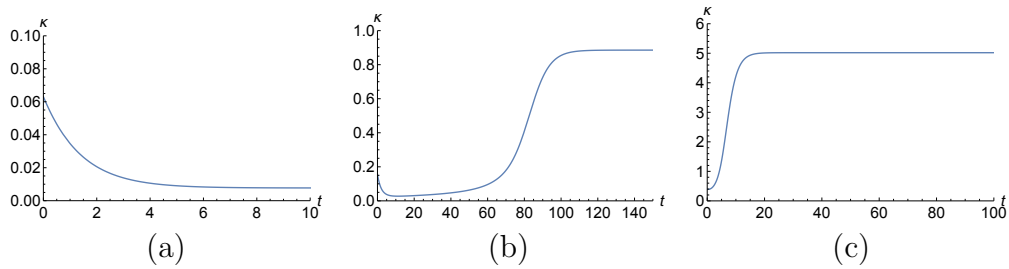

Figure 12: Evolution of shear rate for startup of shear flow for $\epsilon = 0.01$, $\beta = 0.5$, $\delta = -0.5$. (a) $\tau = 0.5$, (b) $\tau = 0.7$, (c) $\tau = 1.0$.

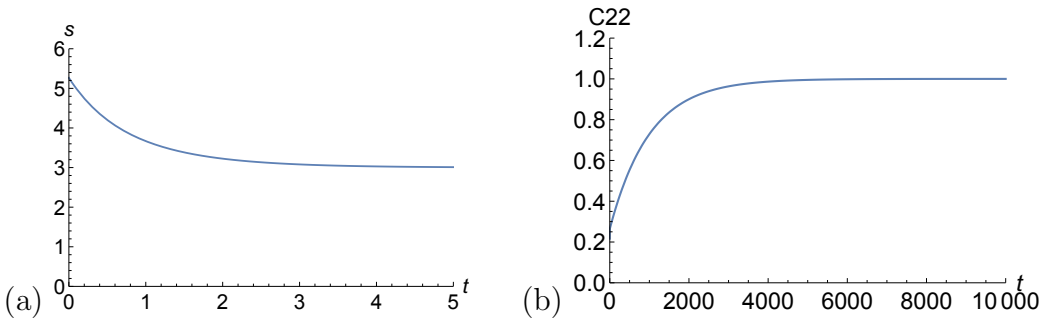

Figure 13: The evolution of s, (a) and C_{22}, (b) after removal of the imposed shear stress. Unyielding from established steady shear flow, $\beta = 0.5$, $\delta = -0.5$. The initial shear flow is for $\tau = 1$.

In particular, we have obtained the following results:

- In startup of shear flow with a given imposed stress, the flow remains unyielded at low stresses and yield immediately at sufficiently high stresses. In an intermediate regime, delayed yielding occurs: The flow appears to settle to an unyielded regime, but it continues to evolve slowly and eventually yields. The stretching and non-stretching versions of the model behave similarly.

- In cessation of shear flow, the molecular configuration returns to equilibrium on the slow timescale. This leads to thixotropy: While the molecules remain deformed, the yield stress and apparent viscosity on subequent loading remain diminished. The degree of thixotropy is highly sensitive to convective constraint release. This finding may suggest experimental strategies for evaluating the relative importance

of CCR which are more specific than more traditional data fits.

- The exponent δ is most important in the yielded phase, especially at high shear rate. Both positive and negative values lead to shear thinning behavior.

Appendix A: Relative position of points on the slow manifold

This calculation supports the conclusions in Section 2.3. The following results are established:

1. If either $0 \leq \beta < 1$ and $0 < \tau < \sqrt{3/8}$ or $\beta > 1$ and $0 < \tau < \sqrt{3\beta/2}/(1+\beta)$, then $C_{22}^i > C_{22}^{eq} > C_{22}^s$.
2. If $\beta < 1$ and $\sqrt{3/8} < \tau < \sqrt{3/(2(2+\beta))}$, then $C_{22}^i > C_{22}^s$, and C_{22}^{eq} does not exist.
3. If $\beta > 1$, and $\sqrt{3\beta/2}/(1+\beta) < \tau < \sqrt{3/2(2+\beta)}$, then $C_{22}^i > C_{22}^s$, and $C_{22}^s > C_{22}^{eq}$ if C_{22}^{eq} exists.

First of all, we check that, for small τ, we have

$$C_{22}^{eq} \sim 1 - \frac{2}{3}\tau^2, \quad C_{22}^i \sim 1 - \frac{1}{3}\tau^2, \quad C_{22}^s \sim \frac{2}{3}(1+\beta)\tau^2, \tag{51}$$

so clearly $C_{22}^i > C_{22}^{eq} > C_{22}^s$. We next investigate when $C_{22}^{eq} - C_{22}^s$ changes sign. For the equation $C_{22}^{eq} = C_{22}^s$, Mathematica yields the solution $\tau = \sqrt{3\beta/2}/(1+\beta)$. However, this solution pays no attention to the sign of square roots, and a further check reveals that $C_{22}^{eq} - C_{22}^s$ changes sign at this point only if $\beta > 1$. The equation $C_{22}^i = C_{22}^{eq}$ also yields the formal roots $\tau = \sqrt{3\beta/2}/(1+\beta)$. For $\beta < 1$, we find that, at this point, we have actually

$$C_{22}^i = \frac{2+2\beta+\beta^2}{(1+\beta)(2+\beta)} > C_{22}^{eq} = \frac{1}{1+\beta} > C_{22}^s = \frac{\beta}{1+\beta}. \tag{52}$$

On the other hand, for $\beta > 1$, we have

$$C_{22}^i = \frac{2+2\beta+\beta^2}{(1+\beta)(2+\beta)} > C_{22}^s = C_{22}^{eq} = \frac{\beta}{1+\beta}. \tag{53}$$

The other formal root of the equation $C_{22}^i = C_{22}^s$ is $\tau = \sqrt{3/2(2+\beta)}$. At this point, we have $C_{22}^i = C_{22}^s = (1+\beta)/(2+\beta)$, so there is a change of sign. For this value of τ, C_{22}^{eq} does not exist if $\beta < 2$, and we have

$$C_{22}^{eq} = \frac{1}{2}(1 + \sqrt{\frac{\beta-2}{\beta+2}}) < C_{22}^s \tag{54}$$

if $\beta \geq 2$.

Now we apply these results to startup of flow. Consider solutions starting from equilbrium along a fast curve and entering the slow dynamics at $C_{22} = C_{22}^i$ as given in (16). Since C_{22}^i is larger than either the equilibrium values C_{22}^{eq} or the singular value C_{22}^s, the numerator of (19) is negative and the denominator is positive. Therefore, C_{22} decreases until it reaches either equilibrium or the singular value. Finally, one of the following two scenarios must take place:

1. If $0 \leq \beta < 1$ and $0 < \tau < \sqrt{3/8}$ or $\beta > 1$ and $0 < \tau < \sqrt{3\beta/2}/(1+\beta)$, the equilibrium point C_{22}^{eq} is ultimately reached via slow dynamics. This is unyielded behavior.
2. If $\beta < 1$ and $\sqrt{3/8} < \tau < \sqrt{3/(2(2+\beta))}$, or $\beta > 1$, and $\sqrt{3\beta/2}/(1+\beta) < \tau < \sqrt{3/(2(2+\beta))}$, the singular point is reached along the slow manifold. At this point, the dynamics transitions to another fast curve, along which yielded equilibrium is reached. This is the case of delayed yielding. The delay time is essentially equal to the residence time along the slow manifold, i.e. it is of order $1/\epsilon$.

Appendix B: Stability of the yielded fixed point and unyielding

The purpose of this appendix is to discuss in more detail the dynamics in the neighborhood of the fixed point $C_{22} = C_{22}^0 = \beta/(1+\beta)$, $C_{12} = C_{12}^0 = \sqrt{3\beta/2}/(1+\beta)$ for the fast dynamics (12). For this purpose, we expand to the next order in ϵ. We set $C_{12} = C_{12}^0 + \epsilon c_{12}$, $C_{22} = C_{22}^0 + \epsilon c_{22}$, substitute into the full equations, and linearize in ϵ. For $\beta \neq 0$, this leads to

$$\begin{aligned}
(1+\beta)\dot{c}_{12} &= 2(\beta - \frac{1}{3}\sqrt{6\beta}\tau(1+\beta))c_{12} + ((1+\beta)\tau - \frac{1}{2}\sqrt{6\beta})c_{22} - \frac{1}{2}\sqrt{6\beta}, \\
(1+\beta)\dot{c}_{22} &= (\beta - \frac{1}{3}\sqrt{6\beta}\tau(1+\beta))c_{22} + 1.
\end{aligned} \tag{55}$$

We refer to these equations as "yielded dynamics." For the nonstretching case, the yielded dynamics is just simply the linearization at the yielded steady flow. This is different, however, for the full Rolie-Poly model. Yielded dynamics given by (55) has the fixed point

$$\begin{aligned} c_{12} &= \frac{9(1-\beta)}{2\sqrt{6}\beta(-3\sqrt{\beta}+\sqrt{6}(1+\beta)\tau)}, \\ c_{22} &= \frac{3}{-3\beta+\sqrt{6\beta}(1+\beta)\tau}. \end{aligned}$$

This represents yielded steady flow up to order ϵ.

The eigenvalues of the matrix representing the linear system (55) are $\beta/(1+\beta) - \frac{1}{3}\sqrt{6\beta}\tau$ and $2(\beta/(1+\beta) - \frac{1}{3}\sqrt{6\beta}\tau)$. Therefore, the fixed point exists and is stable as long as $\tau > \sqrt{3\beta/2}/(1+\beta)$. We note that, regardless of τ, the fixed point is on the line

$$c_{12} = \frac{3(1-\beta)}{2\sqrt{6\beta}} c_{22}. \tag{56}$$

Now we consider what happens if the initial condition is this yielded steady flow and the imposed shear stress τ is suddenly decreased. If the new τ is higher than $\sqrt{3\beta/2}/(1+\beta)$, then the solution of (55) will simply approach the new fixed point. If, on the other hand, the new τ is below $\sqrt{3\beta/2}/(1+\beta)$, then the fixed point is unstable, and the solution of (55) will go to infinity.

To discuss the latter case further, the direction of approach to infinity in the (c_{12}, c_{22})-plane must be found. Let us assume that for $t < 0$, we have steady yielded flow, and the fixed point for (55) is given by (c_{12}^a, c_{22}^a). For $t > 0$, τ is set to a lower value, such that the new fixed point (c_{12}^b, c_{22}^b) is unstable. Let $d_{12} = c_{12} - c_{12}^b$, $d_{22} = c_{22} - c_{22}^b$. Then the evolution for $t > 0$ is given by

$$\begin{aligned} (1+\beta)\dot{d}_{12} &= 2(\beta - \frac{1}{3}\sqrt{6\beta}\tau(1+\beta))d_{12} + ((1+\beta)\tau - \frac{1}{2}\sqrt{6\beta})d_{22}, \\ (1+\beta)\dot{d}_{22} &= (\beta - \frac{1}{3}\sqrt{6\beta}\tau(1+\beta))d_{22}, \end{aligned} \tag{57}$$

and the initial condition is

$$d_{12}(0) = c_{12}^a - c_{12}^b, \quad d_{22}(0) = c_{22}^a - c_{22}^b. \tag{58}$$

We have $c_{22}^a > 0$, $c_{22}^b < 0$, so $d_{22}(0) > 0$. Moreover, according to (56),

$$d_{12}(0) = \frac{3(1-\beta)}{2\sqrt{6\beta}} d_{22}(0). \tag{59}$$

In the phase plane for (57), the origin is an unstable node; the analysis of the eigenvectors shows that the fast direction is given by the d_{12} axis, and the slow direction can be shown to be given by the line $d_{12} = \sqrt{6}/(2\sqrt{\beta})d_{22}$. The initial point given by (59) is always to the left of this line. It follows that for $t \to \infty$, the solution of (57) will be such that d_{12} is negative and $|d_{12}| >> |d_{22}|$.

The system (57) agrees with the linearization of the fast dynamics at the yielded fixed point $C_{12} = \sqrt{3\beta/2}/(1+\beta)$, $C_{22} = \beta/(1+\beta)$. The solution of (55) which we just discussed naturally matches to the line $C_{22} = \beta/(1+\beta)$, which is an invariant line under the fast dynamics given by (12). Upon unyielding, the solution follows this line until either $C_{12} = \tau$ is reached or, if τ is sufficiently negative, C_{12} approaches $-\sqrt{3\beta/2}/(1+\beta)$, i.e. there is a yielded flow in the opposite direction.

At the point where $C_{12} = \tau$ is reached, C_{22} is still close to $\beta/(1+\beta)$. It will then slowly relax following the slow manifold, i.e. over a time scale of order $1/\epsilon$.

Appendix C: Slow dynamics for the full Rolie-Poly model with $\delta = 0$.

The analysis of slow dynamics begins with adding a correction to the stretch near equilibrium: $\operatorname{tr}\mathbf{C} = C_{11} + 2C_{22} = 3 + \epsilon d$, $\kappa = \epsilon\tilde{\kappa}$, where d is the rescaled stretch to be determined. Time is rescaled as $t = \tilde{t}/\epsilon$. At leading order, (2) becomes

$$\begin{aligned}
\frac{dC_{22}}{d\tilde{t}} &= 1 - C_{22} - \frac{d}{3}(C_{22} + \beta(C_{22} - 1)), \\
C_{22}\tilde{\kappa} &= \tau(1 + \frac{d}{3}(1+\beta)), \\
d &= 2\tau\tilde{\kappa}.
\end{aligned}$$

We find

$$d = \frac{6\tau^2}{3C_{22} - 2(1+\beta)\tau^2},$$

$$\tilde{\kappa} = \frac{3\tau}{3C_{22} - 2(1+\beta)\tau^2}, \tag{60}$$

and C_{22} obeys the same equation as (19) derived above for the slow dynamics of the nonstretching Rolie-Poly model.

In contrast to the nonstretching case, there is no closed form expression for C_{22}^i, the initial value of C_{22} where fast dynamics transitions to slow dynamics in startup of shear flow. However, some qualitative properties follow. First, the transition from fast to slow dynamics must occur at $s = 3$ and $ds/du < 0$ in (29). This implies that

$$C_{22}^i > C_{22}^s = 2(1+\beta)\tau^2/3, \tag{61}$$

where C_{22}^s is the singular value defined in (21). In the nonstretching case, we showed that when there are equilibrium points, then C_{22}^i is bigger than the larger of the two equilbrium values. We have no proof of this in the stretching case, but for our conclusions below, it suffices to show that $C_{22}^i > 1/2$, the average of the two equilibrium values. In conjunction with the above result that $C_{22}^i > C_{22}^s$, and the obvious fact that $C_{22}^i > \beta/(1+\beta)$, this guarantees that as long as there is a stable equilibrium value for C_{22} in the range $1 > C_{22} > \beta/(1+\beta)$, the solution on the slow manifold will converge to that equilibrium value. We have $C_{22}^i > \beta/(1+\beta) > 1/2$ if $\beta > 1$. The remaining case is $\beta \leq 1$ and $\tau^2 \leq 3/8$. We consider the solution (30), determine u such that $C_{22} = 1/2$, and compute the corresponding s. The result is

$$s = \frac{3}{2} + \tau^2 \frac{\beta(2+5\beta+\beta^2) + 2(1-\beta^2)\ln(1-\beta)}{2\beta^2}. \tag{62}$$

A contour plot (which we omit) shows that this value is less than or equal to 3 in the range $0 \leq \beta \leq 1$, $0 \leq \tau^2 \leq 3/8$, with equality only when $\beta = 1$, $\tau^2 = 3/8$. Therefore, the value $s = 3$ is reached before C_{22} gets to $1/2$.

We can therefore obtain results for startup of steady shear flow which are analogous to the nonstretching case. Specifically, the behavior is as follows:

1. If either $\beta < 1$ and $\tau < \sqrt{3/8}$ or $\beta \geq 1$ and $\tau < \sqrt{3\beta/2}/(1+\beta)$, an unyielded equilibrium is reached via slow dynamics.
2. If $\beta < 1$, $\tau > \sqrt{3/8}$ or $\beta \geq 1$, $\tau > \sqrt{3\beta/2}/(1+\beta)$, but τ is still less than the value given by the upper curve in Figure 7, delayed yielding occurs.
3. If τ is larger than the value given by the upper curve in Figure 7, immediate yielding occurs.

Appendix D: Yielded dynamics for the full Rolie-Poly model with $\delta = 0$.

We now study the dynamics when C_{22} is close to $\beta/(1+\beta)$. We set $C_{22} = \beta/(1+\beta) + \epsilon q$. At leading order in ϵ, we obtain the reduced equation

$$\frac{\beta\kappa}{1+\beta} = 2(1-\sqrt{3/s})(1+\beta)\tau. \tag{63}$$

Using this in the equation for the evolution of s, we find

$$\frac{ds}{dt} = -2(1-\sqrt{3/s})(s+\beta(s-3)) + 4(1-\sqrt{3/s})\frac{(1+\beta)^2\tau^2}{\beta}. \tag{64}$$

Finally, we find

$$\frac{dq}{dt} = \frac{1}{1+\beta} - 2(1-\sqrt{\frac{3}{s}})(1+\beta)q. \tag{65}$$

The equation (64) has the equilibrium points $s = 3$ and

$$s_0 = \frac{3\beta^2 + 2\tau^2(1+\beta)^2}{\beta(1+\beta)}. \tag{66}$$

If $\tau^2 > 3\beta/(2(1+\beta)^2)$, $s_0 > 3$. Moreover, s_0 is stable, and $s = 3$ is unstable. If $\tau^2 < 3\beta/(2(1+\beta)^2)$, then $s_0 < 3$, and the stability conditions are reversed. If we start from a yielded steady shear flow and then lower the value of τ, the flow will remain yielded if $\tau^2 > 3\beta/(2(1+\beta)^2)$, but it will unyield and transition to slow dynamics if τ^2 is less than this value.

Acknowledgment

This research was supported by the National Science Foundation under Grants DMS-1311707 and DMS-1514576. The authors would like to thank the Department of Mathematics, University of British Columbia, for their hospitality during the time when this manuscript was written.

[1] J.M. Adams and P.D. Olmsted, Nonmonotonic models are not necessary to obtain shear banding phenomena in entangled polymer solutions, *Phys. Rev. Lett.* **102** (2009), 219802.

[2] J.M. Adams, S.M. Fielding and P.D. Olmsted, Transient shear banding in entangled polymers: a study using the Rolie-Poly model, *J. Rheol.* **55** (2011), 1007-1032.

[3] H.A. Barnes and K. Walters, The yield stress myth?, *Rheol. Acta* **24** (1985), 323-326.

[4] F. Caton and C. Baravian, Plastic behavior of some yield stress fluids: from creep to long-time yield, *Rheol. Acta* **47** (2008), 601-607.

[5] D. Hinrichsen and A.J. Pritchard, *Mathematical Systems Theory I*, Springer Texts in Applied Mathematics, 2005.

[6] R.G. Larson, A constitutive equation for polymer melts based on partially extending strand convection, *J. Rheol.* **28** (1984), 545-571.

[7] R.G. Larson, Constitutive equations for thixotropic fluids, *J. Rheol.* **59** (2015), 595-611.

[8] A.E. Likhtman and R.S. Graham, Simple constitutive equation for linear polymer melts derived from molecular theory: RoliePoly equation, *J. Non-Newt. Fluid Mech.* **114** (2003), 1-12.

[9] K.L. Maki and Y. Renardy, The dynamics of a viscoelastic fluid which displays thixotopic yield stress behavior, *J. Non-Newt. Fluid Mech.* **181-182**, 30-50.

[10] R.L. Moorcroft and S.M. Fielding, Shear banding in time-dependent flows of complex fluids, *Phys. Rev. Lett.* **110** (2013), 086001.

[11] M. Renardy, The mathematics of myth: Yield stress behavior as a limit of nonmonotone constitutive theories, *J. Non-Newt. Fluid Mech.* **165** (2010), 519-526.

[12] P. Tapadia and S.Q. Wang, Yieldlike constitutive transition in shear flow of entangled polymeric fluids, *Phys. Rev. Lett.* **91** (2003), 198301.

[13] P. Vasquez, L.P. Cook and G.H. McKinley, A network scission model for wormlike micellar solutions I: model formulation and homogeneous flow predictions, *J. Non-Newt. Fluid Mech.* **144** (2007), 122-139.

[14] S.Q. Wang, Comment on nonmonotonic models are not necessary to obtain shear banding phenomena in entangled polymer solutions, *Phys. Rev. Lett.* **103** (2009), 219801.